# DYNAMIC THERMOGRAPHY DERIVED PERFUSION AS A POTENTIAL TOOL FOR EVALUATING CUTANEOUS PERFUSION CHANGES IN RESPONSE TO LOW-LEVEL-LASER IRRADIATION

By

VASUMATHI CHALASANI

Bachelor of Science in Electronics and Communication

Jawaharlal Nehru Technological University

Hyderabad, Andhra Pradesh, India

2012

Submitted to the Faculty of the
Graduate College of the
Oklahoma State University in
partial fulfillment of
the requirements for the
Degree of MASTER OF
SCIENCE May, 2014

DYNAMIC THERMOGRAPHY DERIVED

PERFUSION AS A POTENTIAL TOOL FOR

EVALUATING CUTANEOUS PERFUSION CHANGES

IN RESPONSE TO LOW-LEVEL-LASER

IRRADIATION

Thesis Approved:

Dr. Piao, Daqing

Thesis Advisor

Dr. Bartels, Kenneth

Dr. Chandler, Damon

# ACKNOWLEDGMENTS

I would like to offer my sincere gratitude to my advisor, Dr. Daqing Piao, for his continuous guidance, support, patience, and motivation. This thesis would not have been possible without all the inputs from him. I am grateful to Dr. Kenneth E. Bartels for his insights and for financially supporting my research and Dr. Damon Chandler for his kind encouragement and insights. I would like to thank my lab mates for all their discussions and feedback. I would like to thank my family and friends for their support, love and understanding without which this work would not have been possible.

Name: Vasumathi Chalasani

Date of Degree: MAY, 2014

Title of Study: DYNAMIC THERMOGRAPHY DERIVED PERFUSION AS A POTENTIAL TOOL FOR EVALUATING CUTANEOUS PERFUSION CHANGES IN RESPONSE TO LOW-LEVEL-LASER IRRADIATION

Major Field: Electrical Engineering

Purpose and Method of Study: The objective of this study is to develop method for extracting cutaneous perfusion information from dynamic thermography, using an improved bio-heat transfer model for the initial application to study the responses of cutaneous perfusion to low level laser irradiation. The bio-heat transfer model developed in this study for dynamic thermography-derived perfusion employs the contributions of heat transfer due to blood circulation, which has been implemented in previous models, and a spatial Laplacian term accounting for heat changes due to conduction, which has been neglected by previous models. The model is applied to dynamic thermography imagery obtained at 23Hz of frame rate from cutaneous tissues of turtle subjects and human volunteers subjected to the same laser irradiation protocol of 20 seconds of irradiation between 20 seconds of idle time prior to and after the laser irradiation.

Results and Conclusion: The proposed method yields stable results over all 6 sets of human data with a perfusion range similar to that estimated from other cited works whereas the other models falter for 3 or more sets of data. For turtle data the perfusion pattern is similar to that by the other models attributable to the low changes in heat conduction pertaining to their thermoregulation mechanism. The algorithm is being implemented in a Graphical-User-Interface (GUI) for the clinical testing by physicians.

TABLE OF CONTENTS

Chapter Page

LIST OF TABLES

LIST OF FIGURES

Figure Page

Figure Page

Nomenclature

| **Parameter** | **Unit** |
|---|---|
| Temperature | K |
| Mass | Kg |
| Length | m |
| Volume | ml |
| Time | s |
| Energy | J |

| **Symbol** | **Description** | **Units** |
|---|---|---|
| $C_{blood}$ | Specific heat of blood | J/[Kg.K] |
| $C_{tissue}$ | Specific heat of tissue | J/[Kg.K] |
| $\rho_{blood}$ | Mass density of blood | Kg/ml |
| $\rho_{tissue}$ | Mass density of tissue | Kg/ml |
| $\omega_{blood}$ | Rate of blood perfusion | ml/[60s.0.1Kg] |
| $T_b$ | Blood temperature in core | K |
| $T_s$ | Skin Temperature | K |
| $\kappa$ | Thermal Conductivity of Skin | J/[m.s.K] |
| d | Depth of core temperature point from cutaneous surface | m |
| $Q$ | Heat change as a result of temperature changes | J/s |
| $Q_b$ | Heat change as a result of convection due to blood flow | J/s |
| $Q_c$ | Heat change as a result of conduction by subcutaneous tissue | J/s |

# CHAPTER I

## INTRODUCTION

### I.1 Perfusion:

Blood perfusion is the volumetric flow of blood through the capillaries and extra cellular spaces of the body. It is defined as the rate of blood flow per amount of tissue per time. Hence it is measured in ml/100g.min.This flow is microscopic. At the perfusion level nutrients are carried by the blood and exchanged with cells and wastes are carried away. It is estimated that there are 10 billion capillaries in the human body and every cell is at least within 20 to 30 micrometers from one another. Perfusion is thus intrinsic to the healthy functioning of the body and therefore its quantification can be of great use to medicine and health care [1].

In addition to transporting fuel and wastes to and from cells, blood circulation is also a mechanism of heat transfer. Blood flow brings heat from the core of the body to the extremities. If a thermal event is applied to a tissue, blood perfusion will dissipate the applied heat or reheat a cooled area. However, the heat transfer through the tissue cannot be modeled with perfusion alone. Other parameters like thermal conductivity and specific heat of the tissue also affect the temperature distribution which when calculated and modeled can be used to measure blood perfusion. Therefore by measuring the temperature response of the tissue and modelling some of the related parameters as a bio-

heat model, which is shown in later parts, can be used to deduce a value for blood perfusion.

## I.2 Low-level laser therapy

With the invention of the laser in1960, a new direction of medical treatment emerged. The usage of laser to induce heat for medical purposes became common. By inducing a temperature elevation of a few degrees above the body temperature the laser was used as a method to treat tumors and other harmful lesions in the human body. The advantage of using laser light for thermotherapy with other methods is due to the fact that it deposits, a precise amount of energy in a well-defined region, inducing lesions of reproducible size in a minimally invasive way [2].

Low-level laser (or light) therapy (LLLT) also known as cold or soft laser, bio-stimulation, or photo bio-modulation is an emerging medical and veterinary therapeutic approach which uses low-level lasers or light-emitting diodes to either stimulate or inhibit cellular function , leading to reduction of cell and tissue death, improved wound healing, increasing repair of damage to soft tissue, nerves, bone, and cartilage, and relief for both acute and chronic pain and inflammation. Specific test and protocols for LLLT suggest that it is effective in relieving short-term pain for rheumatoid arthritis, osteoarthritis, acute and chronic neck pain, tendinopathy, possibly chronic joint disorders, treatment of low back pain, dentistry and wound healing [3].

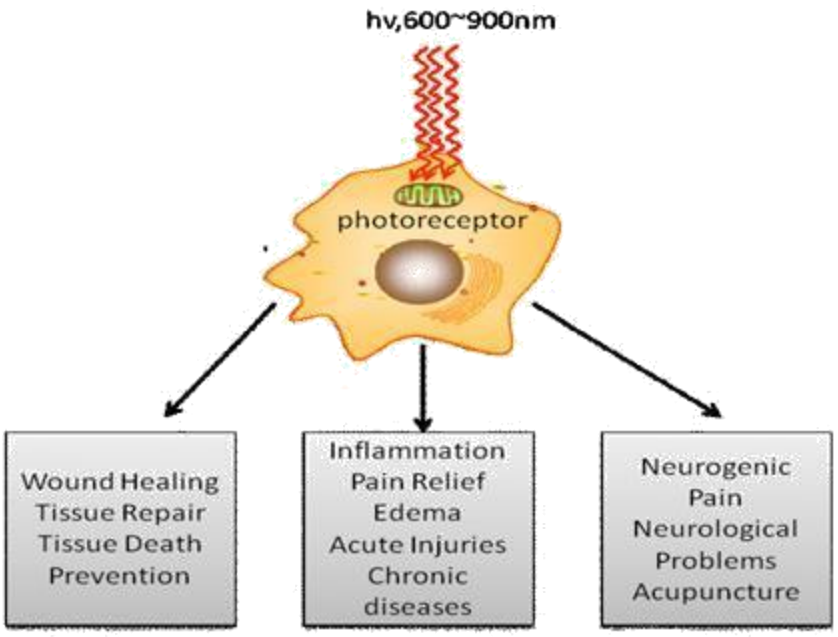


Figure 1: Schematic representation of the main applications of Low-level laser therapy (LLLT) [3].

Shown above in Figure 1 are some main applications for which low-level laser therapy can be used [3].

## I.3 Monitoring Temperature derived perfusion:

Since it has been realized how laser induced thermotherapy plays a significant role in medical treatment, it is important to understand how the tissue will thermally respond during such treatments. This would allow physicians to plan treatment doses and durations for the procedures [4, 5]. The movement of blood, or perfusion, is responsive to the environment. Blood flow increases during activity or trauma to provide necessary nutrients. The cardiovascular system is very dynamic and adjusts to meet the needs of the body. Blood from the core of the body is maintained at a constant 37°C in the human being. If an area of the body becomes warmer or cooler than normal, increased or

decreased perfusion will act to normalize the temperature [6]. If normal tissue is heated by less than several hours, tissue temperature and perfusion are correlated .This increase of tissue perfusion during this period is apparently associated with the release of vasoactive compounds, such as bradykinin, which cause vasodilation [7]. Previous studies have demonstrated that perfusion can be implied from dynamic thermography by applying bio-heat transfer models. In this study we develop a bio-heat transfer model for deriving perfusion information from thermography along the same basis with fewer approximations than the referred previous studies.

I.4 Perfusion value estimates cited from literature

Table 1 gives some estimated Perfusion values from different regions of tissues. These values are obtained from other cited works.

| **Region** | **Perfusion (ml/[(60s)(0.1kg)])** | **Reference** |
|---|---|---|
| Sigmoid colonic tissue | 41.7 ± 7.4 | [8] |
| Tissue | About 40 | [9] |
| Lung tissue | 40.1 | [10] |
| Unheated muscle | 4 to 10 | [10] |
| Brain(gray matter)<br>(white matter) | 70<br>20 | [11] |
| Facial skin mean blood flow(male)<br>(female) | 11.4 ± 2.8<br>7.0 ± 1.6 | [12] |
| Spinal cord blood flow Pre injury case(rats) | 49.7 ± 1.6 | [13] |
| Cuff occlusion(5 min) for human leg | -20 to 50<br>-20 to 80 | [14] |
| Rats- (forepaw at rest)<br>(forepaw with ultrasonic radiation)<br>(hindpaw at rest)<br>(hindpaw with ultrasonic radiation) | 37.17 ± 14.74<br>37.82 ± 14.29<br>35.34 ± 14.77<br>39.28 ± 11.92 | [15] |

Table 1: Perfusion value estimates from literature

## I.5 Thesis Outline

Chapter 2 discusses the bio-heat modelling for thermography derived perfusion in detail, and the literature review performed to complete this work. It covers how the present model was modified based on these papers. Chapter 3 covers the thermal camera operation and laser specifications used to obtain dynamic data. The different protocols followed for imaging real time data from subjects is also provided. Chapter 4 describes the results obtained from the different real time data as three parts. Chapter 5 summarizes the results, discusses the ongoing work (user-friendly GUI) and presents conclusions and suggestions for future work.

# CHAPTER II

## BIO-HEAT TRANSFER MODEL FOR THERMOGRAPHY DERIVED PERFUSION

### II.1 Modeling of bio-heat transfer for thermography derived perfusion

#### i. Heat transfer:

Heat flows in a biological media whenever there is a temperature difference. This transfer of thermal energy is governed by the Laws of Thermodynamics. The two most important principles that are to be considered here are the first and second law of thermodynamics.

The first law of thermodynamics talks about the conservation of energy. It states that the amount of heat lost by regions inside a closed system corresponding to the amount that is gained by the rest of the closed system. The second law talks about the direction of heat flow. It states that the heat flows from regions of higher temperature to lower temperature [2].

At Thermal Equilibrium:

At thermal equilibrium the heat balance equation for human skin tissue can be determined using six factors. These factors are heat radiated from subject to air ($Q_r$), heat due to evaporation ($Q_e$), heat via convection into air neighboring skin surface ($Q_f$), heat conducted by subcutaneous tissue ($Q_c$), heat corresponding to metabolic rate of cutaneous

tissue ($Q_m$ ) and heat via convection attributable to blood flow of subcutaneous blood vessels ($Q_b$ ).These six heat components can be categorized into two groups as heat loss components and heat production components. [16, 17, 18, 19].

- The factors contributing to the loss of heat are:

$Q_r$ : Heat radiated from subject to air,

$Q_e$ : Heat due to evaporation,

$Q_f$ : Heat via convection into air neighboring skin surface,

- The factors contributing to the gain of heat

are: $Q_c$ : Heat conducted by subcutaneous tissue,

$Q_m$ : Heat corresponding to metabolic rate of cutaneous tissue

$Q_b$ : Heat via convection attributable to blood flow of subcutaneous blood vessels

At thermal equilibrium the heat balance equation for skin tissue is given as:

$$Q_r + Q_e + Q_f = Q_c + Q_m + Q_b \qquad [20]$$

Figure 2 shows the six heat transfer: heat production and loss components responsible in maintaining heat balance for skin tissue.

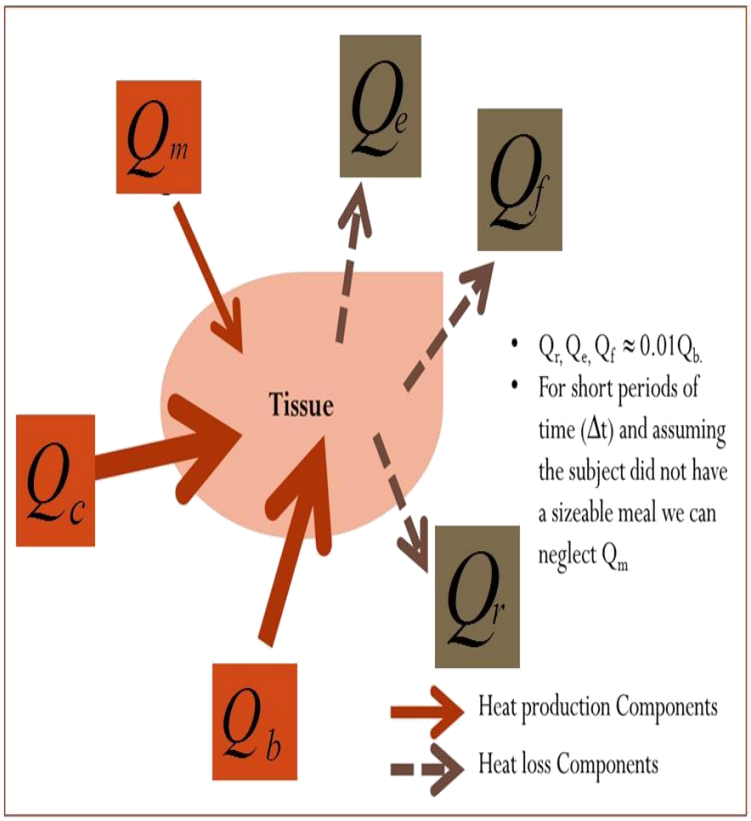


| | |
|---|---|
| $Q_r$ | Heat radiated from subject to air |
| $Q_e$ | Basic evaporated heat |
| $Q_f$ | Heat loss via convection into air neighboring skin surface |
| $Q_c$ | Heat conducted by subcutaneous tissue |
| $Q_m$ | Heat corresponding to metabolic rate of cutaneous tissue |
| $Q_b$ | Heat gain via convection attributable to blood flow of subcutaneous blood vessels |

Figure 2: The heat factors to determine heat balance for skin tissue.

Temperature changes due to heat (ΔQ):

When there are temperature changes the heat production or consumption is unsteady, part of the heat flow will be stored in the control volume. The stored heat will be reflected as temperature changes of the various tissues. The local rate of temperature change is controlled by intrinsic heat capacity (product of density and specific heat) at constant pressure. When it is summed over the tissue control volume the total rate of stored

thermal energy is given by the relation $\Delta Q = \int_V \rho_{tissue} C_{tissue} [\partial T_s(r', t) / \partial t] dV'$ [2]

Heat balance equation for skin tissue due to temperature changes over a short time period Δt can be expressed as:

$$\Delta Q = -(Q_r + Q_e + Q_f) + (Q_c + Q_m + Q_b)$$

- Heat due to radiation ($Q_r$):

Radiation is defined as the transfer of thermal energy via electromagnetic wave action between systems at different temperatures and which are not in contact. This mechanism does not require a medium for its energy transport. In most models of internal biological tissues, the contribution from intrinsic radiative heat transfer process is negligible [21].

Consider a body with temperature $T_b$, the radiation heat flux to the environment with a temperature $T_e$ is given by Stefan-Boltzman law.

$Q_r = \varepsilon\sigma(T_b^4 - T_e^4)$ where $\varepsilon$ is the emissivity and $\sigma$ is Stefan Boltzmann constant.

- Heat due to Evaporation ($Q_e$)

Evaporative heat loss mainly consists of 2 components which are the loss due to respired vapor ($E_{res}$) and evaporative heat loss from skin surface ($E_{sk}$) [22].

$$Q_e = E_{res} + E_{sk}$$

The loss due to respired vapor ($E_{res}$) is given as: $E_{res} = E_{rel} + E_{rec}$ where $E_{rel}$ is the heat loss due to latent respiration and $E_{rec}$ is the heat loss due to convective respiration. The evaporative heat loss from skin surface ($E_{sk}$) is given as: $E_{sk} = E_{dif} + E_{rsw}$ where $E_{dif}$ is

the evaporative heat loss due to skin diffusion and $E_{rsw}$ is the heat loss due to regulatory sweating.

- Heat due to Air Convection($Q_f$)

This heat exchange of air convection can be modeled using Newton's law of cooling [21, 2, 23].Consider a body with temperature $T_b$, the convection heat flux to the environment with a temperature $T_e$ is given as $Q_f = h_f (T_b - T_e)$ where $h_f$ is the coefficient of air convection. It can be calculated as $h_f = \frac{k_f N_u}{d}$ where $K_f$ is thermal conductivity, d is the characteristic length of object, $N_u$ is the Nusselt number. $N_u = A(P_{rr}.G)^M$ where A and M are experimentally determined constants. $P_r$ is Prandtl number which is equal to 0.72 in air, and $G_r$ is Grashof number. On further simplification the convective heat flux due to air is given as: $Q_f = Ak_f d^{3M-1}(P_r g\beta / v^2)^M (T_b - T_e)^{M+1}$ where $g$ is the local gravitational acceleration, $v$ is the kinematic viscosity of air, and ß is the volumetric thermal expansion coefficient of air.

- Heat due to Conduction($Q_c$)

Heat conduction is the transfer of thermal energy through a solid or fluid medium due to an internal temperature gradient. This can be well described by Fourier law of heat conduction. This law states that the amount of thermal energy conducted ($Q_c$) through a medium is directly proportional to the cross-sectional are (A) perpendicular to the heat conduction direction; the temperature difference across the medium ($T_2 - T_1$); the length of time during which conduction occurs (Δt) and inversely proportional to length (d)

across the medium through which heat is conducted which can be neglected for limiting case of infinitesimally small value [2, 21]

$Q_c' = -kA(T_2 - T_1)\Delta t / d$ where K is the proportionality constant called the thermal conductivity. The negative sign shows the second law of thermodynamics which states that heat should flow from regions of higher temperature to lower temperature.

The integral form of fourier law describes $Q_C$ as the rate of heat conduction through the control volume with surface envelope of area dA. It is given as $Q_c = -\int_A K\nabla T_s(r',t).\hat{n}dA'$ where n is unit vector normal to incremental surface area dA'.

- Heat due to metabolism ($Q_m$)

The most widely used approach to estimate metabolic heat production, $Q$m, has been to set this term equal to the oxygen consumption multiplied by the caloric value of oxygen. The heat due to metabolic rate depends on factors like the degree of muscular activities; environmental conditions and body size. Metabolism, as any other chemical reaction, is accelerated with increasing temperature as long as the higher temperature does not lead to the inhibition of the metabolic process by, for example, the denaturation of enzymes. The temperature dependence can be written as $Q_m = Q_{mo}(1.1^{\Delta T})$ where $Q_{mo}$ is the basal metabolic heat production rate and $\Delta T$ is the temperature increase. The basal metabolic heat production rate is highly variable, ranging approximately 5 W/m$^3$ for subcutaneous fat and 50 kW/m$^3$,for working muscle. Compared with the heating rate when using a laser for heat treatment, the metabolic heat production can be neglected [23].

- Heat due to blood Convection($Q_b$)

From the viewpoint of thermal physiology, the skin, tissues, and especially the fat of the subcutaneous tissues are heat insulators. The insulation beneath the skin is an effective means of maintaining normal core temperature, even though it allows the skin temperature to approach the ambient temperature. Conversely, blood vessels penetrate the subcutaneous tissues and are profusely distributed beneath the skin. Much research from biology and bioengineering has demonstrated that the main mechanism of heat exchange from deep body to skin is by circulation of blood [2, 21].

The most common approach to analyze the important effect of blood perfusion on the tissue energy balance is based on the application of Fick's principle. It states that "the amount of substance taken up by an organ or control volume per unit time is equal to the arterial level of the substance minus the venous level times the rate of blood flow".

$$Q_b' = \rho_{blood} C_{blood} \rho_{tissue} \omega_{blood} (T_b - T_s)$$

When the entire tissue control volume is considered, the total amount of thermal energy transported by the blood stream becomes

$$Q_b = \int_V \rho_{blood} C_{blood} \omega_{blood} \rho_{tissue} [T_b(r',t) - T_s(r',t)] dV'$$

ii. Deriving the perfusion term:

For short periods of time (Δt) and assuming the subject did not have a sizeable meal we can neglect $Q_m$. The terms $Q_r$, $Q_e$, $Q_f$ are approximately 1/100 times less than the magnitude of $Q_b$. Hence these terms can also be neglected. [16,17].

So the simplified energy balance equation can be written as:

$$\Delta Q = Q_c + Q_b$$

$$\Delta Q = \int_{r', V} \rho_{tissue} C_{tissue} [\partial T_s(r', t) / \partial t] dV$$

$$Q_c = -\int_A K \nabla T_s(r', t).\hat{n} dA' \quad ,$$

$$Q_b = \int_V \rho_{blood} C_{blood} \omega_{blood} \rho_{tissue} [T_b(r', t) - T_s(r', t)] dV'$$

$$\int \rho_{tissue} C_{tissue} [\partial T_s(r', t) / \partial t] dV' = -\int K \nabla T_s(r', t).\hat{n} dA' + \int \rho_{blood} C_{blood} \omega_{blood} \rho_{tissue} [T_b(r', t) - T_s(r', t)] dV' \quad V A V$$

By applying the divergence theorem to the above equation can be simplified as:

$$\rho_{tissue} C_{tissue} [\partial T_s(r', t) / \partial t] = -\nabla [K \nabla T_s(r', t)] + \rho_{blood} C_{blood} \omega_{blood} \rho_{tissue} [T_b(r', t) - T_s(r', t)]$$

$$\rho_{tissue} C_{tissue} [\partial T_s(r', t) / \partial t] + K[\nabla^2 T_s(r', t)] = \rho_{blood} C_{blood} \omega_{blood} \rho_{tissue} [T_b(r', t) - T_s(r', t)]$$

$$\omega_{blood} = \frac{\rho_{tissue} C_{tissue} [\partial T_s(r', t) / \partial t] + K[\nabla^2 T_s(r', t)]}{(\rho_{blood} C_{blood} \rho_{tissue} [T_b(r', t) - T_s(r', t)])}$$

## II.2. Comparing proposed modeling with previous studies

The idea of using bio-heat modelling to obtain derived perfusion from temperature was inspired from [16], [17], [18] and [19]. Temperature measurement is widely used in the assessment of cutaneous circulation. Therefore, monitoring of cutaneous temperature ($T_S$) and its distribution by means of thermal infrared imaging (IR) has been proposed and

used for the indirect assessment of possible microvascular or cutaneous tissue impairments [16,17,18,19].

i. Reference model :1 (from [16] and [17])

The analytical equation of the perfusion related term from the bio-heat model is given as the time derivative of the blood-flow rate.

$$\frac{a\omega_{blood}}{dt} = \frac{Cons\tan t}{([T_b(r',t) - T_s(r',t)])^2}\frac{\partial T_s}{\partial t}$$

where Constant value given by $C - Kc/3d$ and acts like a scale factor.

The expression can be integrated numerically over time to obtain an estimate for the perfusion (blood flow rate).

ii. Reference model :2 (from [19] )

The perfusion related term from the bio-heat model is determined as:

$$\omega_{blood} = \frac{C_{tissue}[\partial T_s(r',t)/\partial t]}{(\rho_{blood} C_{blood}[T_b(r',t) - T_s(r',t)])}$$

iii. Current study

In this study a bio-heat transfer model was developed along the basis of these previous papers with a more rigorous approach and fewer approximations.

The perfusion related term from the bio-heat model per my analytics can be given:

$$\omega_{blood} = \frac{\rho_{tissue} C_{tissue}[\partial T_s(r',t)/\partial t] + K[\nabla^2 T_s(r',t)]}{(\rho_{blood} C_{blood} \rho_{tissue}[T_b(r',t) - T_s(r',t)])}$$

$$\omega_{blood} = \frac{C_{tissue}[\partial T_s(r',t)/\partial t]}{(\rho_{blood} C_{blood} [T_b(r',t) - T_s(r',t)])} + \frac{K[\nabla^2 T_s(r',t)]}{(\rho_{blood} C_{blood} \rho_{tissue} [T_b(r',t) - T_s(r',t)])}$$

In this study I am comparing results from real time in-vivo and simulated data with the analytics given by [16, 17], and [19] with our proposed model. The perfusion related term is given differently in each model and this is summarized and shown in Table 3.

| **Perfusion term ($w_{blood}$) from studies that are being compared** | **Reference** |
|---|---|
| $\omega_{blood} = \frac{Cons\tan t}{[T_b(r',t) - T_s(r',t)]}$ | 1 |
| $\omega_{blood} = \frac{C_{tissue}[\partial T_s(r',t)/\partial t]}{(\rho_{blood} C_{blood} [T_b(r',t) - T_s(r',t)])}$ | 2 |
| $\omega_{blood} = \frac{C_{tissue}[\partial T_s(r',t)/\partial t]}{(\rho_{blood} C_{blood} [T_b(r',t) - T_s(r',t)])} + \frac{K[\nabla^2 T_s(r',t)]}{(\rho_{blood} C_{blood} \rho_{tissue} [T_b(r',t) - T_s(r',t)])}$ | Current study |

Table 2: Comparing the derived perfusion related term from different studies.

- Thermal Camera Specifications [16]:

Thermal IR imaging has been performed by using a 3–5μm digital infrared camera (AEG Aim GmbH, Heilbronn, Germany), with 0.02 second time resolution, 0.1 K temperature sensitivity, and 0.02 K temperature noise. Emissivity of the skin was estimated as ≅ 0.95.

- Thermal Camera Specifications [17]:

They used a cooled mid-infrared camera, the Radiance HS by Raytheon. The focal plane area (FPA) of the camera is sensitive to the 3-5μm waveband and its size is 256 × 256 pixels.

By observing these equations we can see that the reference model: 1 just considers a scaled temperature value as its perfusion term. Reference model: 2 and Current study give a better approximation of the perfusion term by considering other key parameters along with the change in temperature. To compare Reference model: 2 and Current study, a true image is created similar to that of real-time thermal in-vivo obtained in our study(shown in the latter part).The models are processed on these images to observe the perfusion change patterns. This part of the work was aimed at trying to analyze the difference between both the models for known conditions. The images as shown in figure 3 and figure 4 were created such that there was a relation to the in-vivo imaging.A horizontal stip of around 40 pixels was creted corresponding to the tissue region. A distorted drop shaped region was also created to resemble a wound. This wound was being partially overlapped by an arrow which depicts the laser used for low-level laser therapy in our study. Images [1] and [2] correspond to the same concept except thatthere is a shift in the laser position in [2] and the wound is surrounded by an artefact of the same high pixel range as the laser.

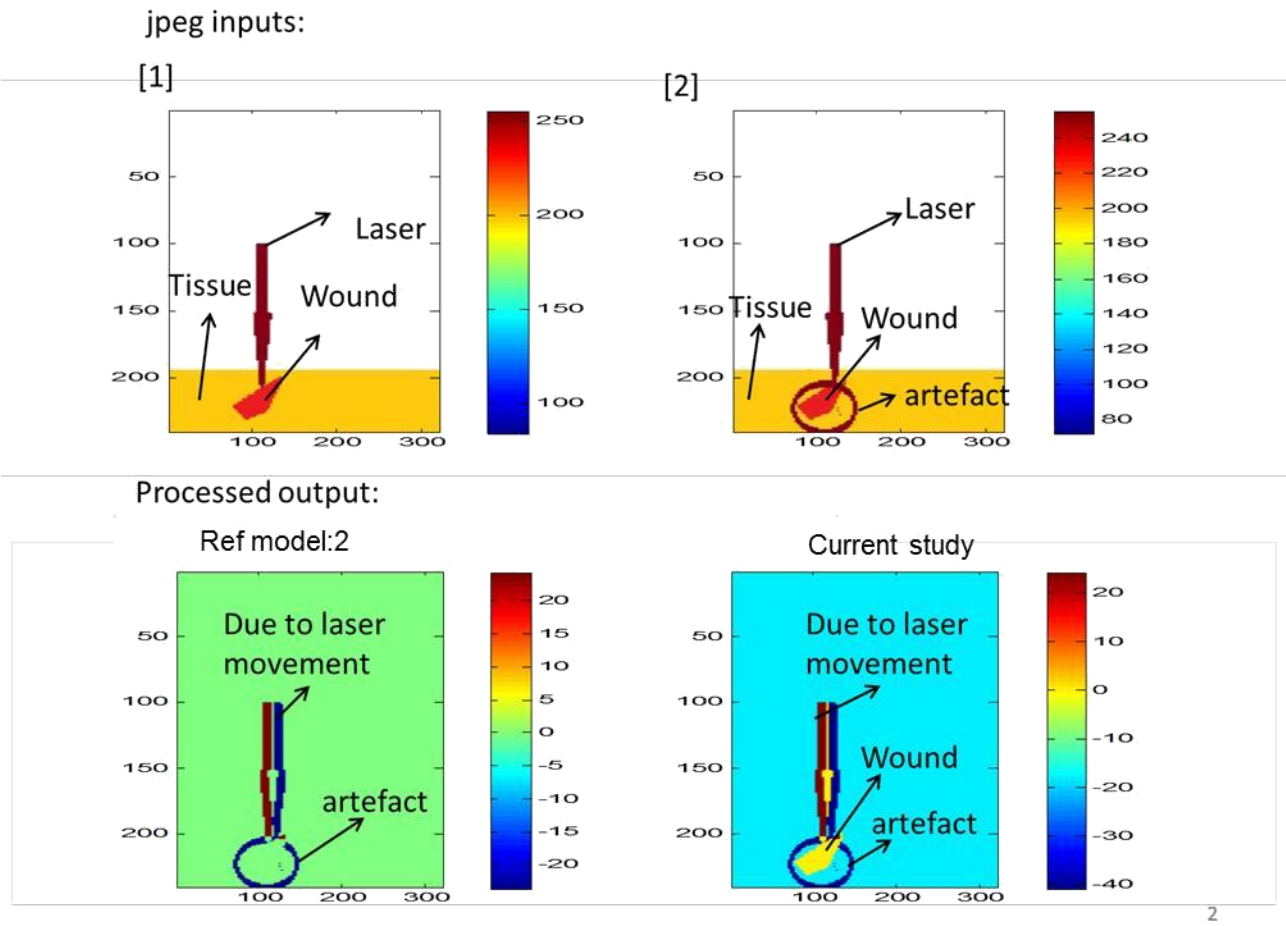


Figure 3: A set of images created to observe the difference between the two models.

In the Processed perfusion the laser and the artefact were displayed in both the models Reference model: 2 and Current study but the wound region appears with a lower scale value in Current study and is not shown at all in Reference model: 2. This is because the wound region is of the same range in both the images so even though it is our area of interest in our imaging and we would like to see the changes happening in that area we cannot observe it from Reference model: 2. This part appears in our model due to the additional scaled laplacian term which is the improvement Reference model: 2 and Current study

Another set of images was created as shown in figure 4 with an additional change.

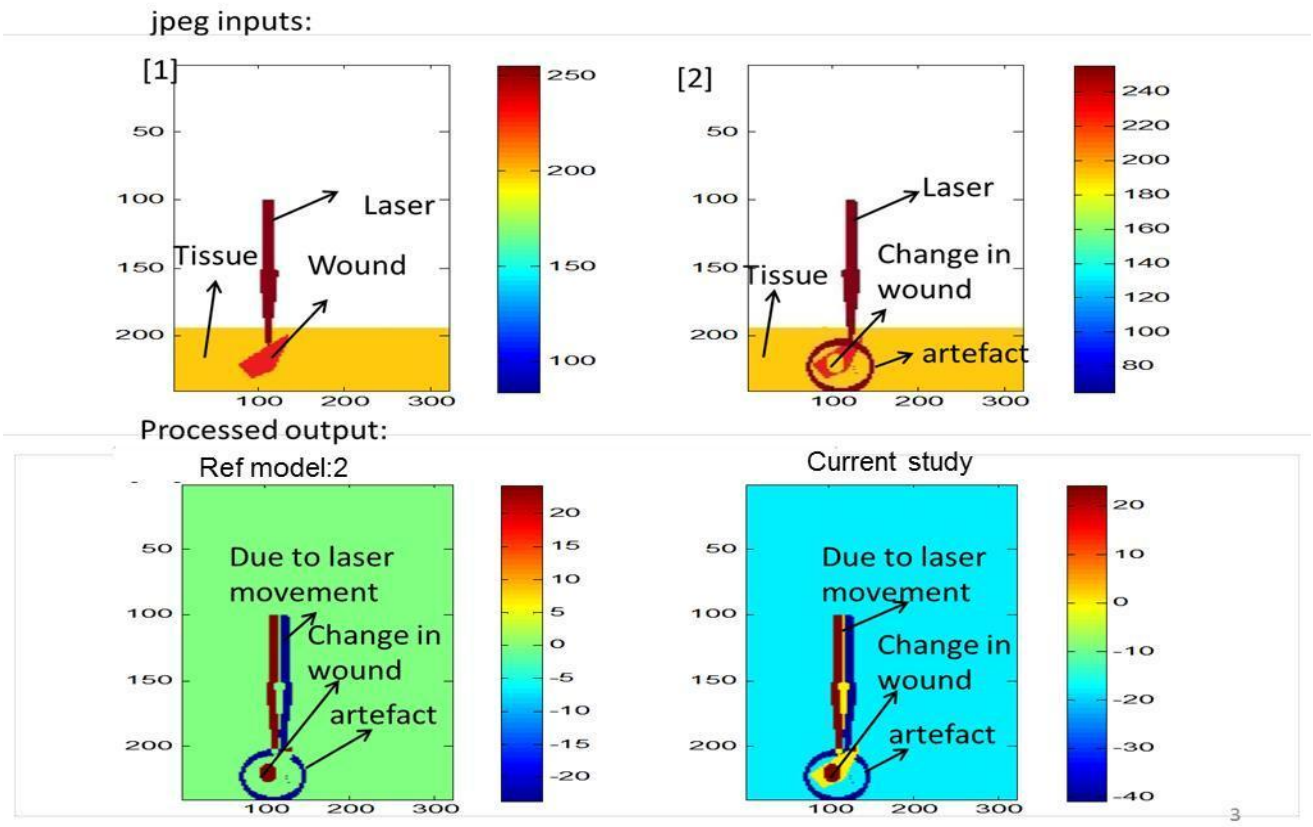


Figure 4: Another set of images created to observe the difference between both models.

In figure 4 the additional change was made in the wound region between the two images so this change was displayed in both the models but the wound area is displayed with the change over a relative scale only in Current study and not in Reference model: 2, thereby helping us visualize the actual changes taking place. The better visualizing and understanding of output between Reference model: 2 and Current study is due to the additional scaled laplacian term in the analytical equation of the perfusion term from the two models.

# CHAPTER III

## METHODOLOGY

### III.1 Thermography equipment and post-processing

An ETIP 7320 P-Series Infrared Camera (Infrared Cameras Inc., Beaumont Tx) with a micro-bolometer 320 x 240 UFPA VOX sensor and a 25mm lens was used for thermography in this study. It is shown in Figure3. The infrared sensor has a spectral response of 8 to 10 μm, a thermal sensitivity of 0.027°C @ 25°C, and an accuracy of ±2°C or ±2%. It is controlled by a laptop computer using USB protocol, with a 16 bits temperature dynamic range. At the default screen resolution of 320 x 240 pixels, the maximum acquisition rate was 23 frames per second. The frames were continuously stored in the dynamic memory during the acquisition, and transferred to hard-drive after the acquisition is stopped. The imaging was done approximately 20" from the subject.

Figure 5: The Infrared Camera used in our study with a controlled laptop

III.2. Laser Specifications:

The laser that was used for low-level laser therapy as part of this study is shown below in Figure 4 with the laser specifications tabulated in Table2:

| | |
|---|---|
| **Laser Type** | Class IV, Solid State |
| **Laser Wavelength** | 980/810 nm |
| **Laser Power** | 0.5W to 15W |
| **Operating Modes** | CW or Pulsed |
| **Aiming Beam** | 650 nm, 5 mW |
| **Dimensions** | 15.6” x 10” x 10.4” |
| **Weight** | 17 lbs. |
| **Power Requirement** | 100 to 240VAC/50-60Hz |
| **Fiber** | Premium, Double-sheathed, Rubber Coated, 800 Microns in diameter |
| **Hand piece** | Finger Switch |

Table 3: Specifications of laser used for low-level laser therapy


Figure 6: The laser used in the study for low-level laser therapy

III.3 Imaging Protocol

i. Laser:

The general Imaging protocol to obtain real time in-vivo data from humans and turtles was to image for 60 seconds with three intervals of 20 seconds having laser off and on over the subject. The schematic is shown in figure 5.


Figure 7: Laser Protocol for 60 seconds

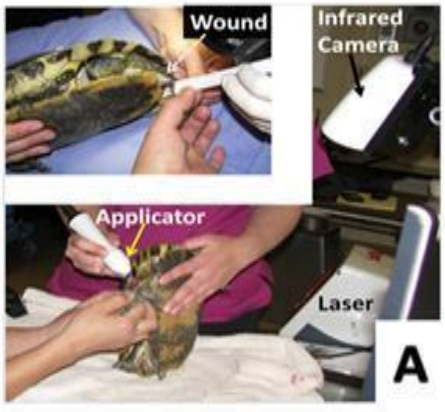


Figure 8: Imaging setup of wounded Turtle with Low-level laser therapy

Shown above in figure 6 is an image which shows a turtle which is being lasered over its wound as part of a treatment, along with the laser being used and the thermal camera which is used for imaging purposes.

The data obtained from human hand was from 6 regions including the right palm, left palm, front of right and left forearm, back of right and left forearm are shown from figure 7 to figure 12

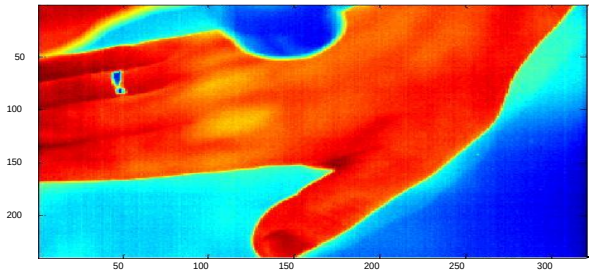


Figure 9: Thermal image from right palm with laser application.

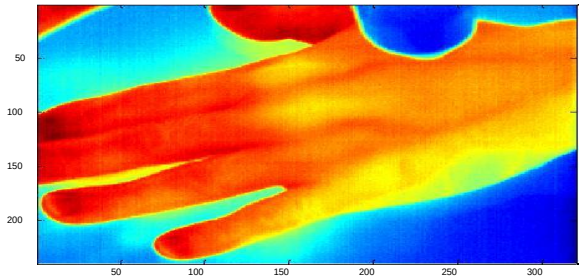


Figure 10: Thermal image from left palm with laser application.

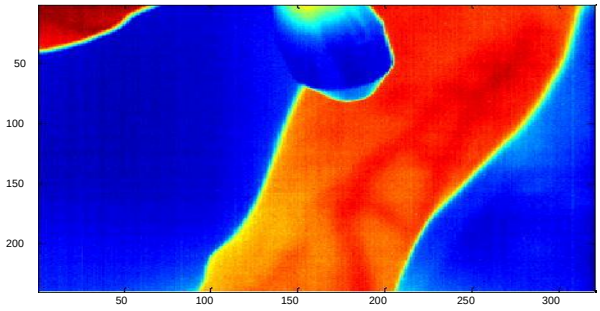


Figure 11: Thermal image from right forearm with laser application.

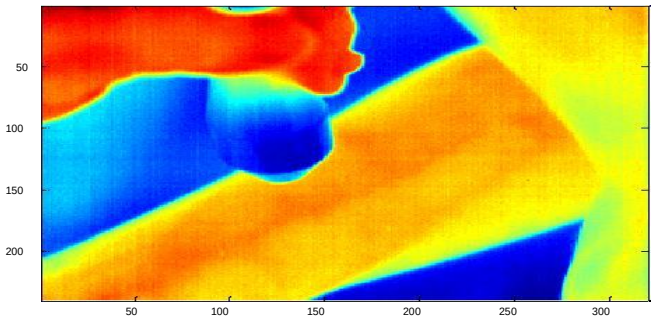


Figure 12: Thermal image from left forearm with laser application

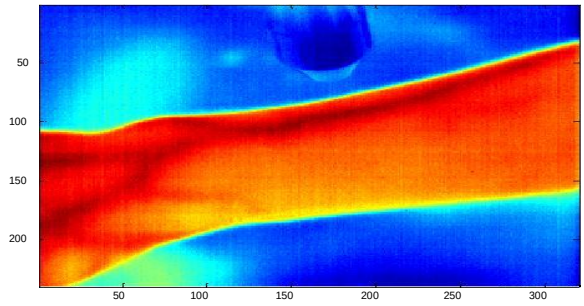


Figure 13: Thermal image from back of left forearm with laser application.

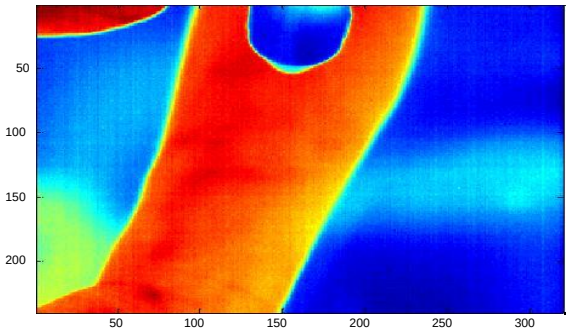


Figure 14: Thermal image from back of right forearm with laser application.

The data was obtained from both legs of 3 turtles. Shown in figure 13 is one such image.

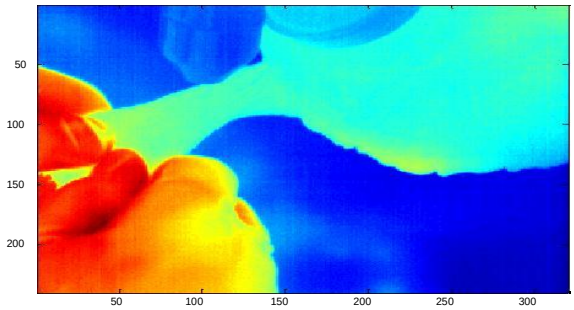


Figure 15: Thermal image from turtle leg with laser application.

ii. Pressure Cuffing

The general Imaging protocol to obtain real time in-vivo data from turtles was to image for 60 seconds with 3 intervals of not applying and applying pressure cuff. This protocol is shown in figure 14 with a schematic.

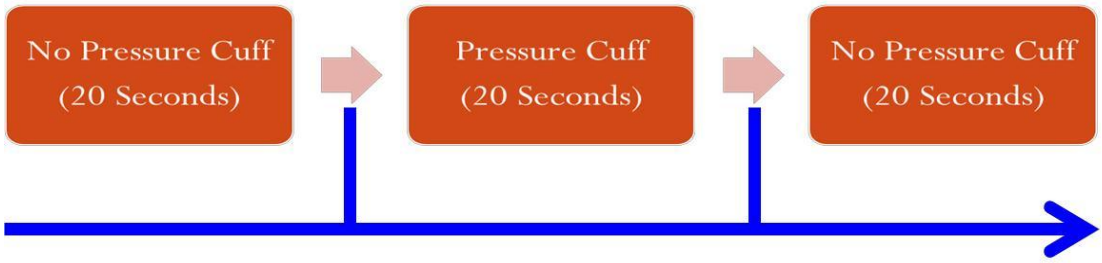


Figure 16: Pressure cuffing Protocol for 60 seconds

The data was obtained from both legs of 4 turtles. Shown in figure 15 is one such image.

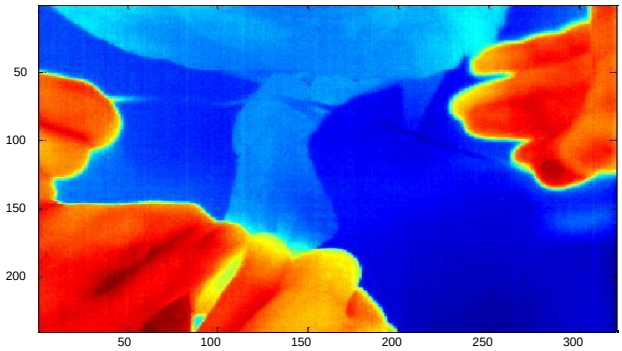


Figure 17: Thermal image from turtle leg with application of pressure cuff

The reason for conducting the pressure cuffing protocol image was that we expected some significant change in perfusion during the application and the release of the pressure cuff.

# CHAPTER IV

## RESULTS

The results of this study are categorized into three parts. All the data are obtained real time from humans and turtles as per the protocols mentioned in the Methodology section. The first part shows the different results from the analytical modelling of the bio-heat model by Reference model: 1, 2 and Current study for the non-tissue region. Here the laser head which, interferes the heated tissue region is considered. In second part the different data from the tissue region of lased and pressure cuffed thermal data are processed using the analytical bio-heat model by Reference model: 1, 2 and Current study. The third part compares the perfusion pattern obtained from processing real time data of lasing humans and turtles.

### IV.1 Part-1: Comparing different models on in-vivo data from non-tissue region

In Chapter 2 a true condition data was generated using tissue and laser and wound region. This data was processed using the different models to observe the difference in the output perfusion pattern. In this part of the study a few sets of human data which had a significant interference of the laser head and the heated tissue region where selective thresholding was not applicable were considered. The presence of the laser head and its overlapping with the tissue region hinders in observing the perfusion pattern. The different models proposed by Reference model: 1, 2 and Current study, are compared in figures 18 and 19.

Ref model: 1

Ref model: 2

Current study

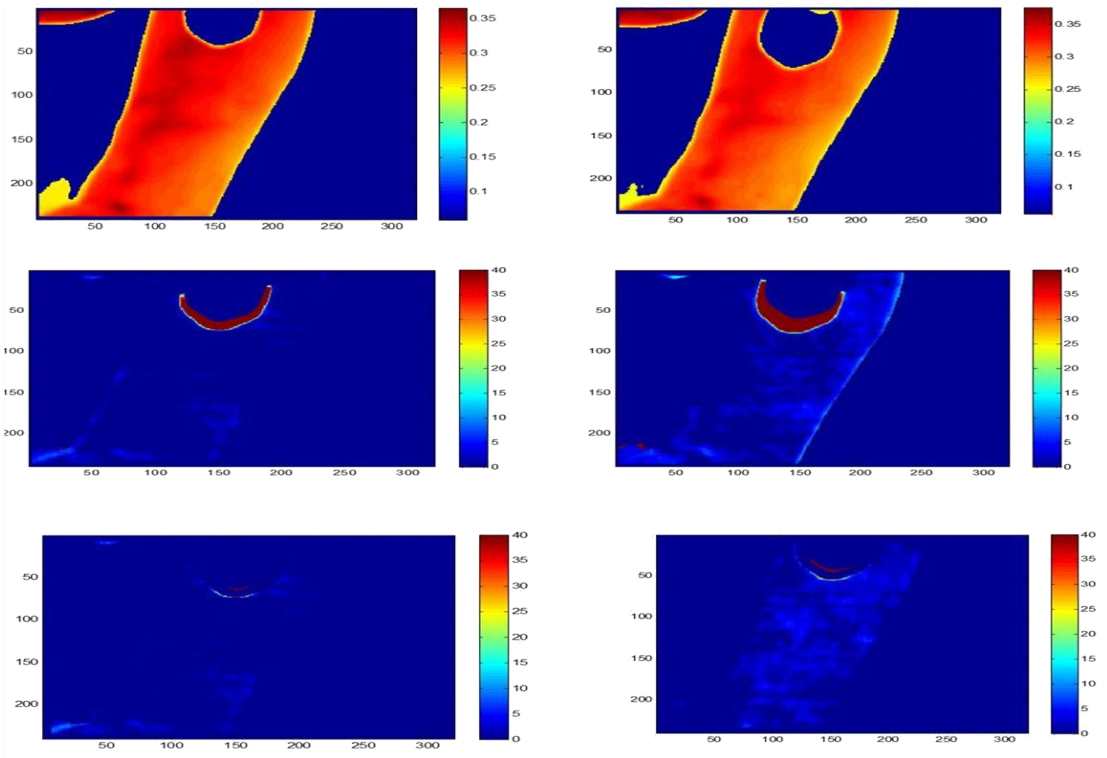

Figure 18: Output Perfusion images from different models (non-tissue region)

Ref model: 1

Ref model: 2

Current study

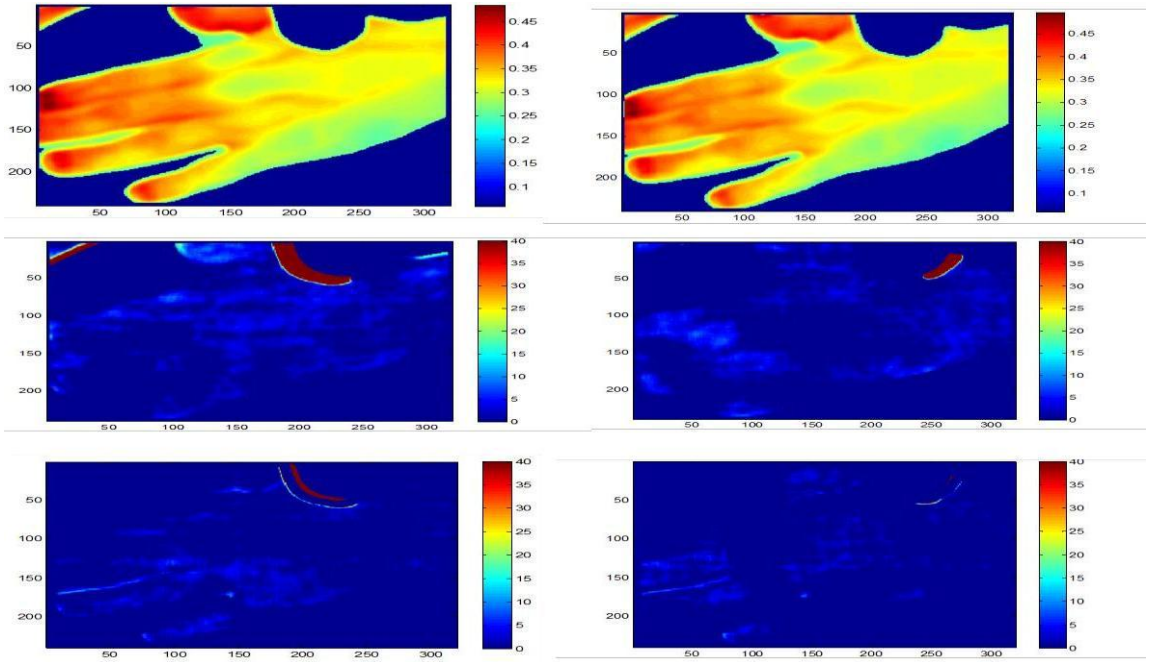

Figure 19: Another set of Output Perfusion images from different models (non-tissue region)

In figures 18 and 19 we can observe the different degrees of laser head edges popping up in the output data from different models. The output from [Reference model: 1] displays a clear edge of laser in the midrange in both figures. Results from [Reference model: 2] show a significant amount of laser head and edges at maximum perfusion range in both the figures. Results from [Current study] show a very small amount of laser head and edges at maximum perfusion range in both the figures thereby showing an improvement from both the previous models.

IV.2 Part-2: Comparing different models on in-vivo data from tissue region

The perfusion pattern from the forepaw and hindpaw of rats due to ultrasonic radiation from [15] is shown below in figure 20.

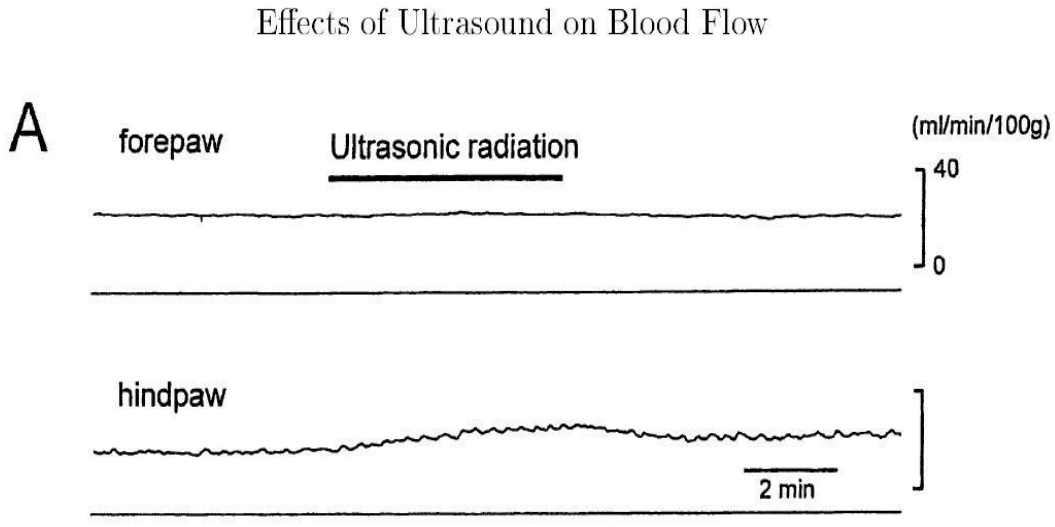


Figure 20: The perfusion output pattern on endotherms due to Ultrasound from [15]

This pattern can be compared with the output pattern obtained from our study with the human data attributing to the endotherm nature of both the species.

To show the different results obtained from the analytical modelling of the bio-heat model by [16, 17], [19] and proposed model the procedure followed was as follows: Selective thresholding was applied to all applicable data in order to eliminate possible artefacts, but in certain situations this thresholding technique was not applicable and so data was processed without it [24].The maximum temperature changes in the lased region over the subject is selected as the Region of Interest (ROI). These values are plotted over time to show the maximum temperature change over time. This is shown in the first part of figure. Over the same ROI the maximum values are considered as a narrower ROI, from the perfusion images proposed by each model being discussed. Averaging is done for the narrower ROI for all the outputs and is followed by smoothing. ). These output values are plotted over time to show the average perfusion change over time. The results obtained from Reference model: 1, 2 and Current study using above mentioned method are shown in the latter part of the figure respectively. A similar procedure is followed for the pressure cuffed data without the smoothing procedure.

i. From Lasing of Human hand.

Figures 21 to 26 shown below correspond to the outputs discussed above for 6 sets of data obtained from the lasing action over different parts of the human hand from our study.

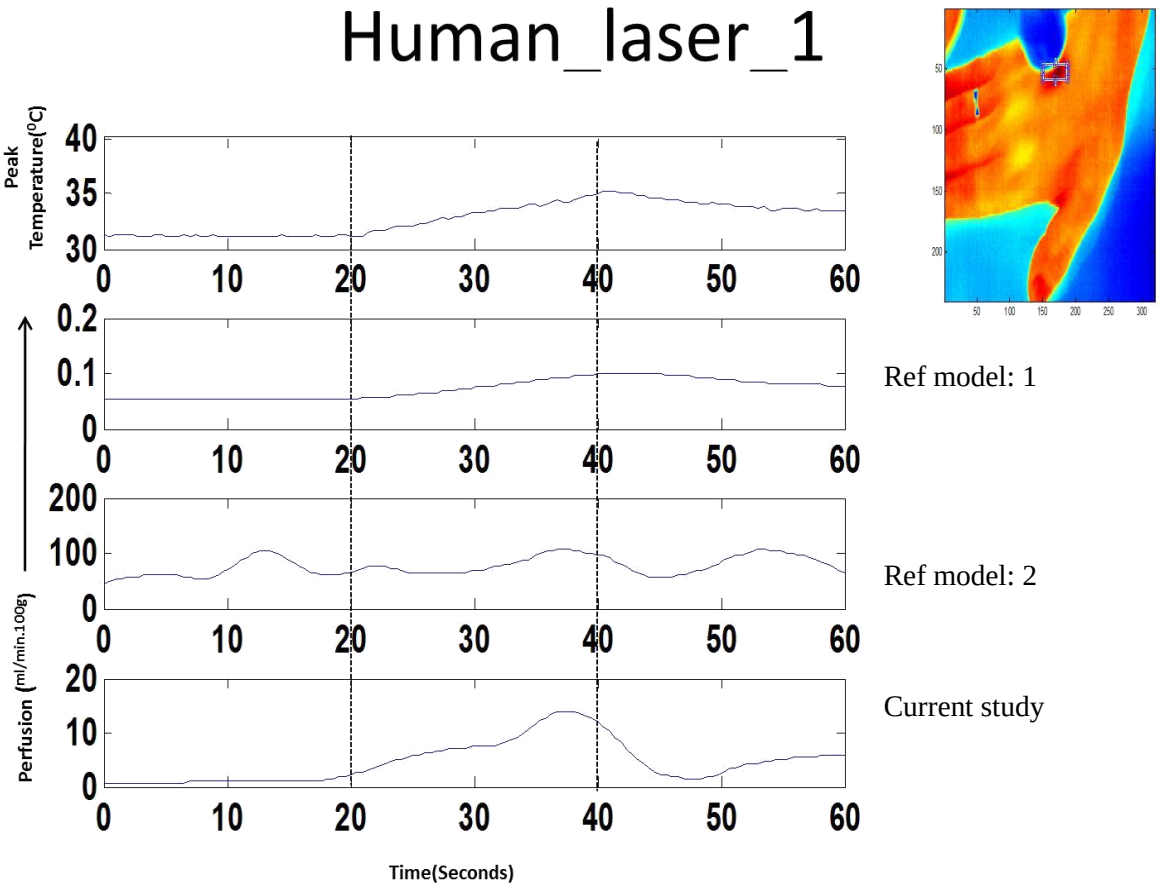


Figure 21: Temperature and Perfusion values from in-vivo data of right palm with laser.

The results obtained from this set of data shown in figure 21 show that:

Reference model: 1 displays perfusion output as a scaled temperature input. Reference model: 2 displays the perfusion output at a much higher range than the true value with unstable variations over non-lased duration. Current study displays a more stable perfusion output at the documented range of values with a significant change during laser irradiation period, else stable changes.

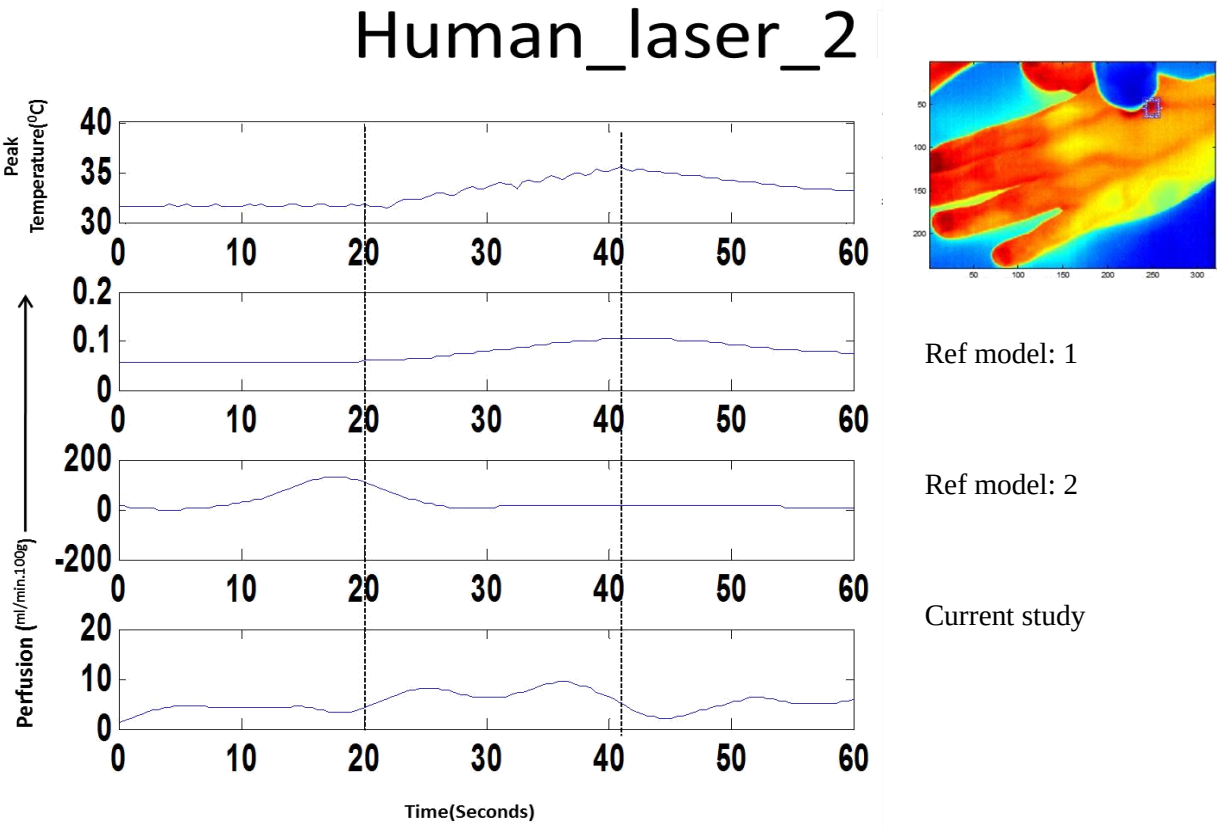


Figure 22: Temperature and Perfusion values from in-vivo data of left palm with laser.

The results obtained from this set of data shown in figure 22 show that:

Reference model: 1 displays perfusion output as a scaled temperature input. Reference model: 2 displays a significant perfusion change at a much higher range than the actual values before the laser irradiation and almost constant pattern at lasing interval. Current study displays a more stable perfusion output showing significant change during laser irradiation period at the documented range of perfusion values and stable changes otherwise

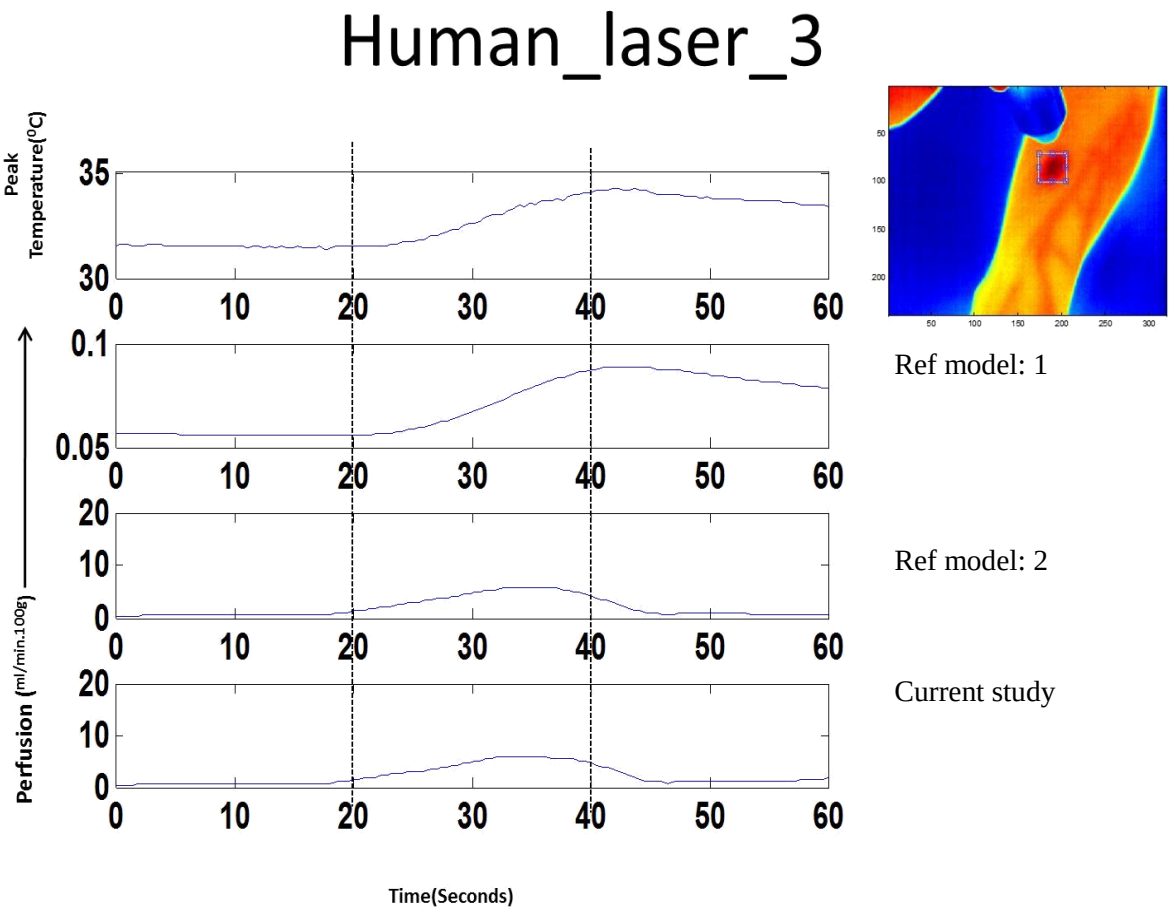


Figure 23: Temperature and Perfusion values from in-vivo data of right forearm with laser.

The results obtained from this set of data shown in figure 23 show that:

Reference model: 1 displays perfusion output as a scaled temperature input. In this case Reference model: 2 and current study displays a similar stable perfusion pattern output showing significant change during laser irradiation period and stable changes otherwise. The range of perfusion values are well in the documented range from other studies for both models from this set of data.

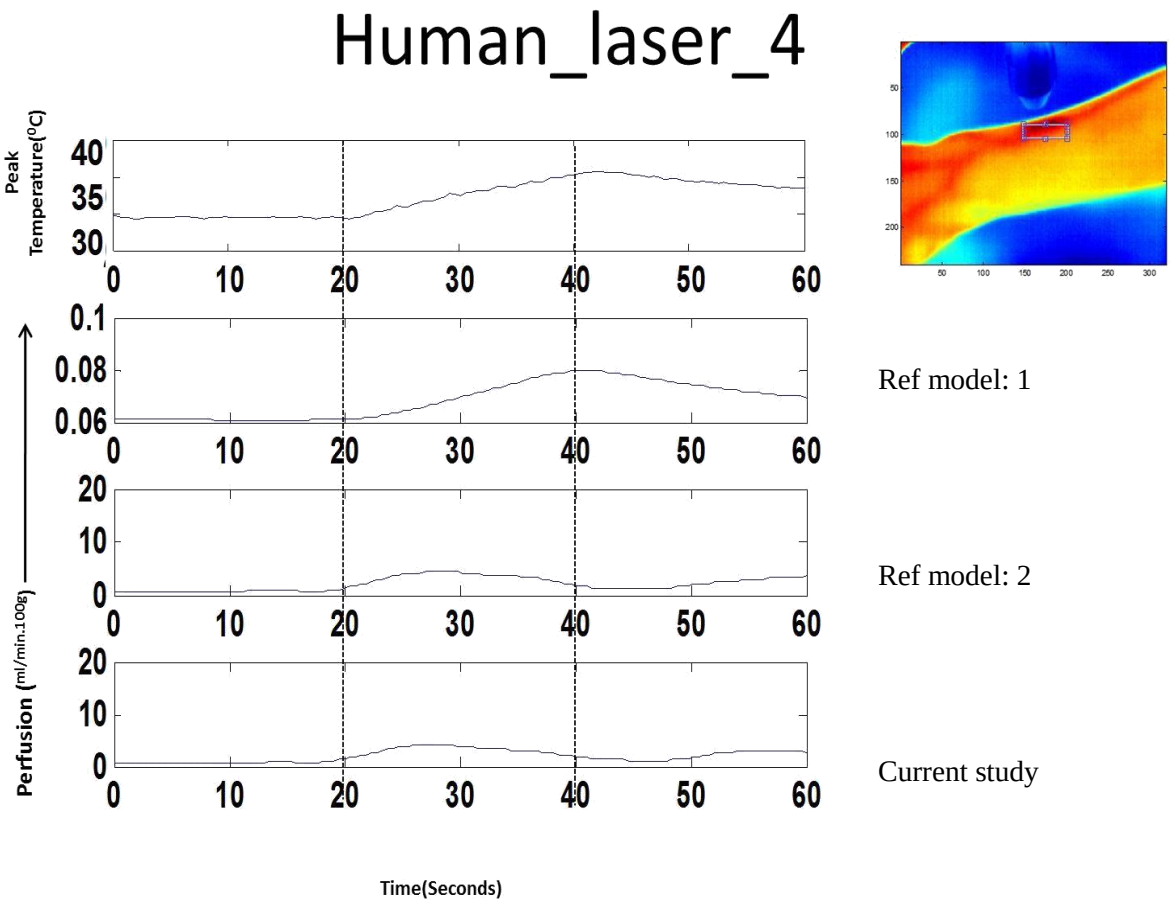


Figure 24: Temperature and Perfusion values from in-vivo data of left forearm with laser application.

The results obtained from this set of data shown in figure 24 show that:

Reference model: 1 displays the perfusion output as a scaled temperature input. In this case Reference model: 2 and current study displays a similar stable perfusion pattern output showing significant change during laser irradiation period and stable changes otherwise. The range of perfusion values are well in the documented range from other studies for both models from this set of data.

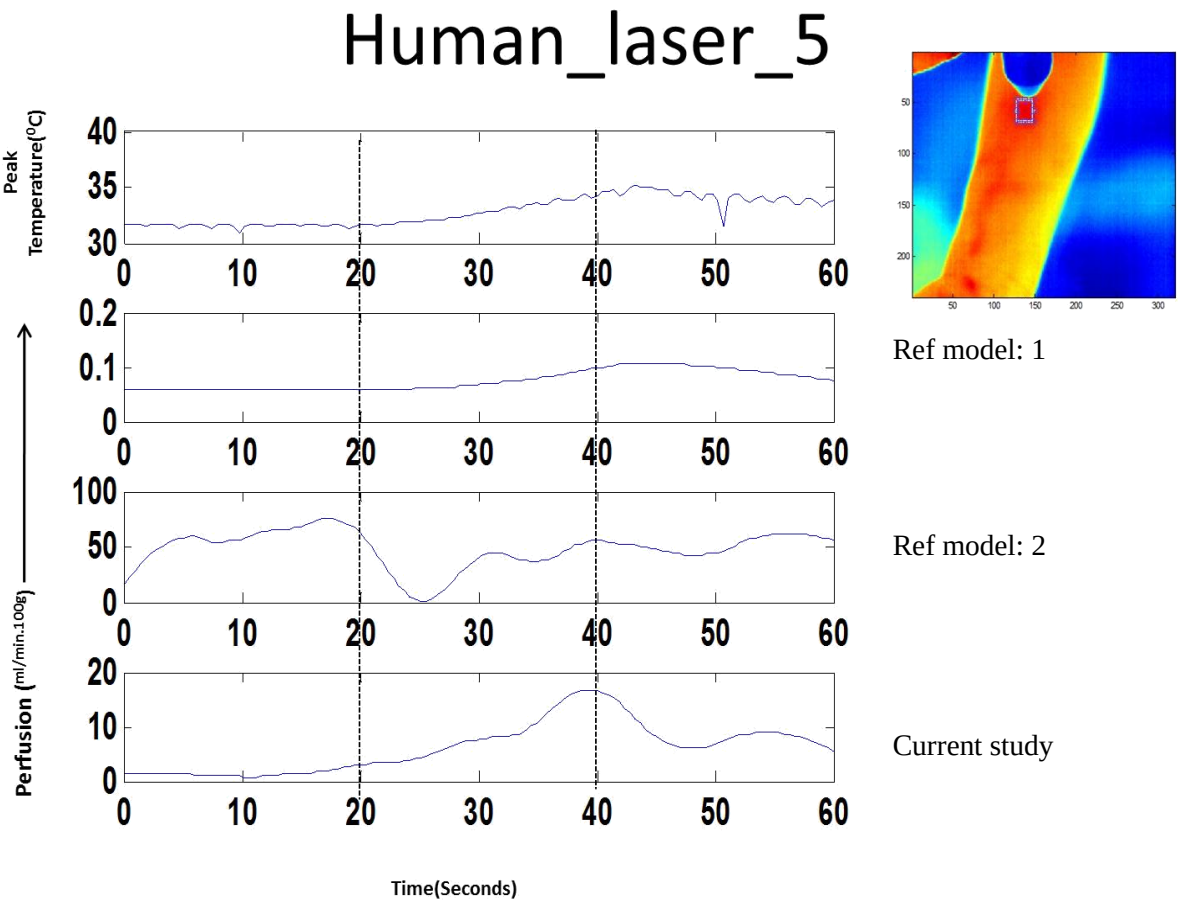


Figure 25: Temperature and Perfusion values from in-vivo data of back of right forearm with laser application.

The results obtained from this set of data shown in figure 25 show that:

Reference model: 1 displays perfusion output as a scaled temperature input. Reference model: 2 displays the perfusion output at a much higher range than the true value with unstable variations over the non-lased duration. Current study displays a more stable perfusion output showing significant change during laser irradiation period and stable changes otherwise at the documented range of perfusion values

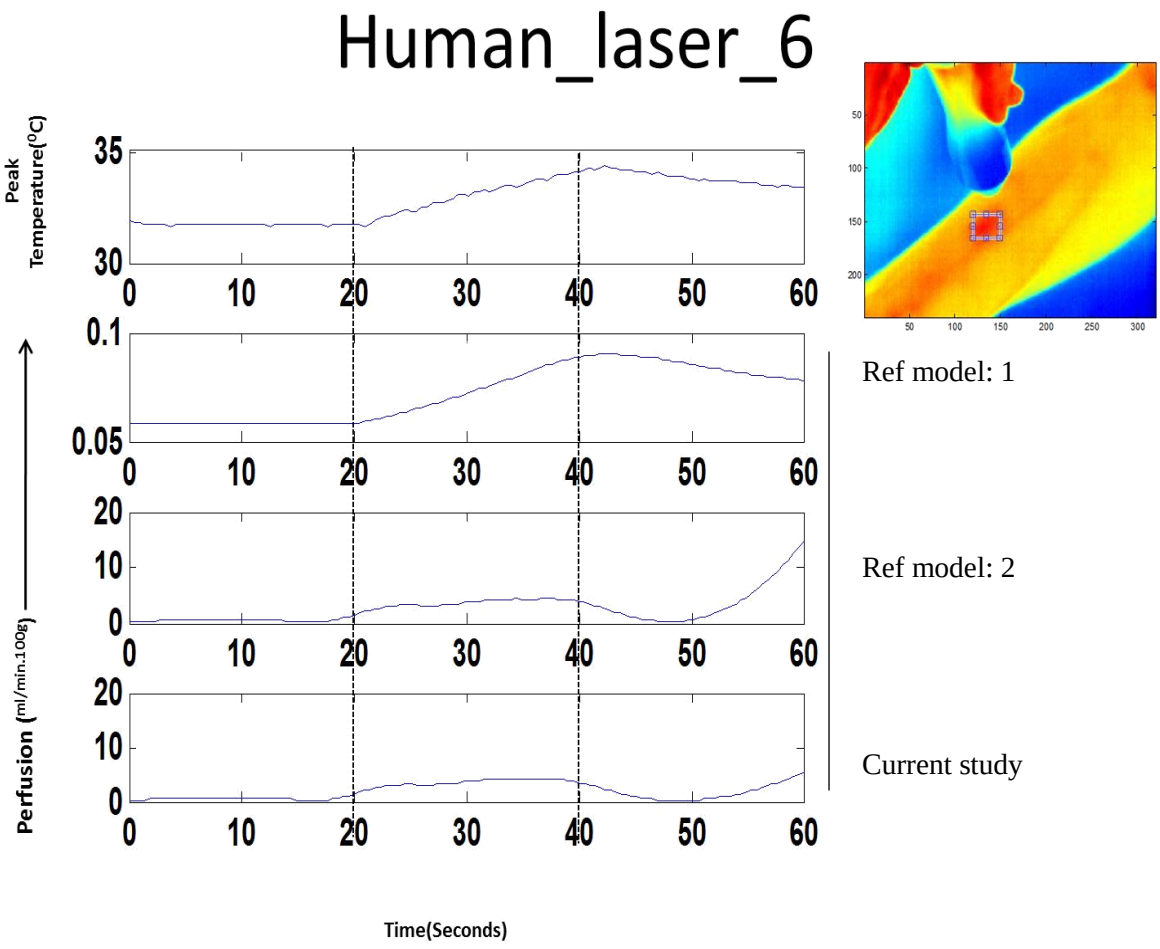


Figure 26: Temperature and Perfusion values from in-vivo data of back of left forearm with laser application.

The results obtained from this set of data shown in figure 26 show that:

Reference model: 1 displays the perfusion output as a scaled temperature input. In this case reference model: 2 and current study display a similar stable perfusion pattern output showing significant change during laser irradiation period and stable changes otherwise. The range of perfusion values are well in the documented range from other studies for both models from this set of data.

ii. From Lasing of Turtles legs.

The perfusion pattern of ectotherms due to thermal changes from [26] is shown below in figure 27. This pattern can be compared with the output pattern obtained from our study with the turtle data attributing to the ectothermic nature of these species.

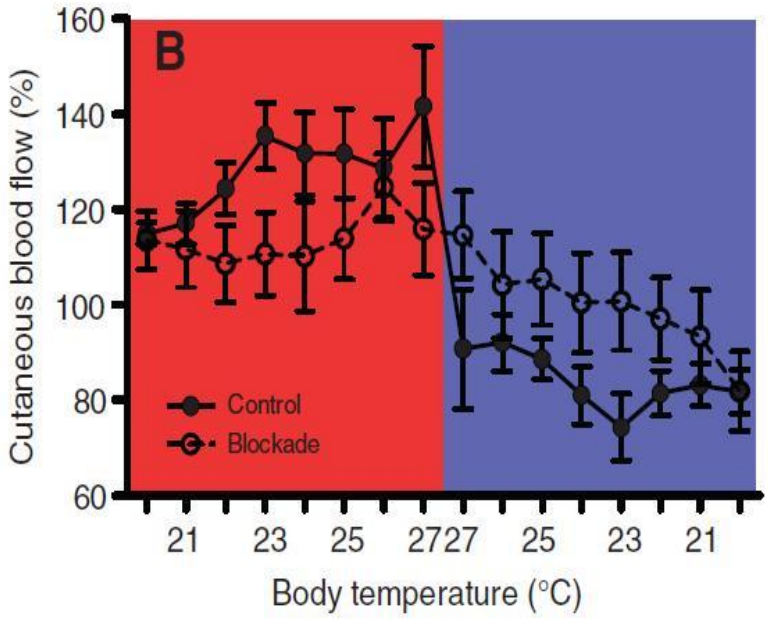


Figure 27: The perfusion output pattern on ectotherms due to Thermal changes from [25]

Figures 28 to 33 shown below correspond to the outputs with the same methodology as that discussed above for lased human data. Here we are comparing the outputs from the 6 sets of data obtained from the lasing action on the legs of turtles.

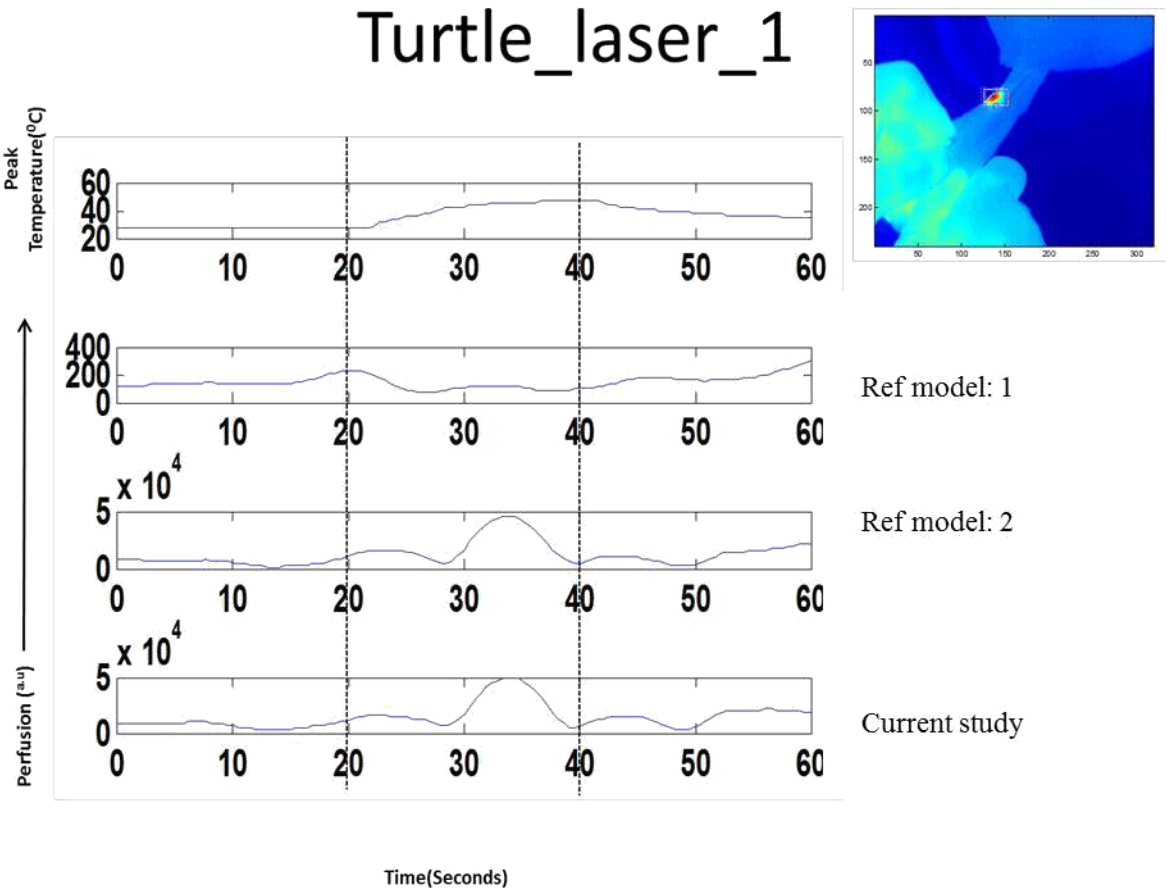


Figure 28: Temperature and Perfusion values from in-vivo data of turtle leg with laser application

The results obtained from this set of data shown in figure 28 show that:

Reference model: 1 displays perfusion output value over a very high range with unstability, irrespective of the laser application. In this case reference model: 2 and current study displays a similar stable perfusion pattern output showing significant change during laser irradiation period and stable changes otherwise. The ranges of perfusion values are much higher than the other sets of data as the region of interest might have included some region from the laser head.

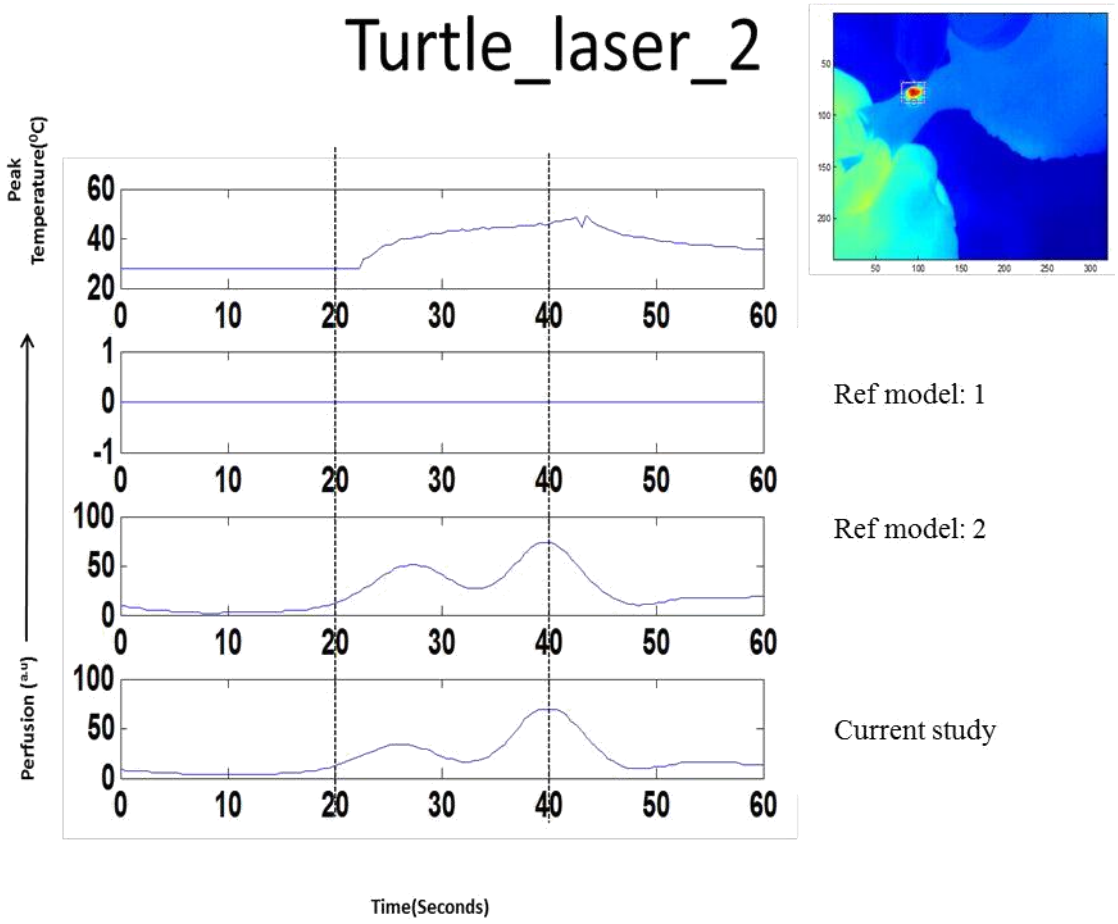


Figure 29: Temperature and Perfusion values from in-vivo data of turtle leg with laser application

The results obtained from this set of data shown in figure 29 show that:

Reference model: 1 displays a zero perfusion output value over the entire 60 second duration, irrespective of the laser application. In this case reference model: 2 and current study displays a similar stable perfusion pattern output showing significant change during laser irradiation period and stable changes otherwise.

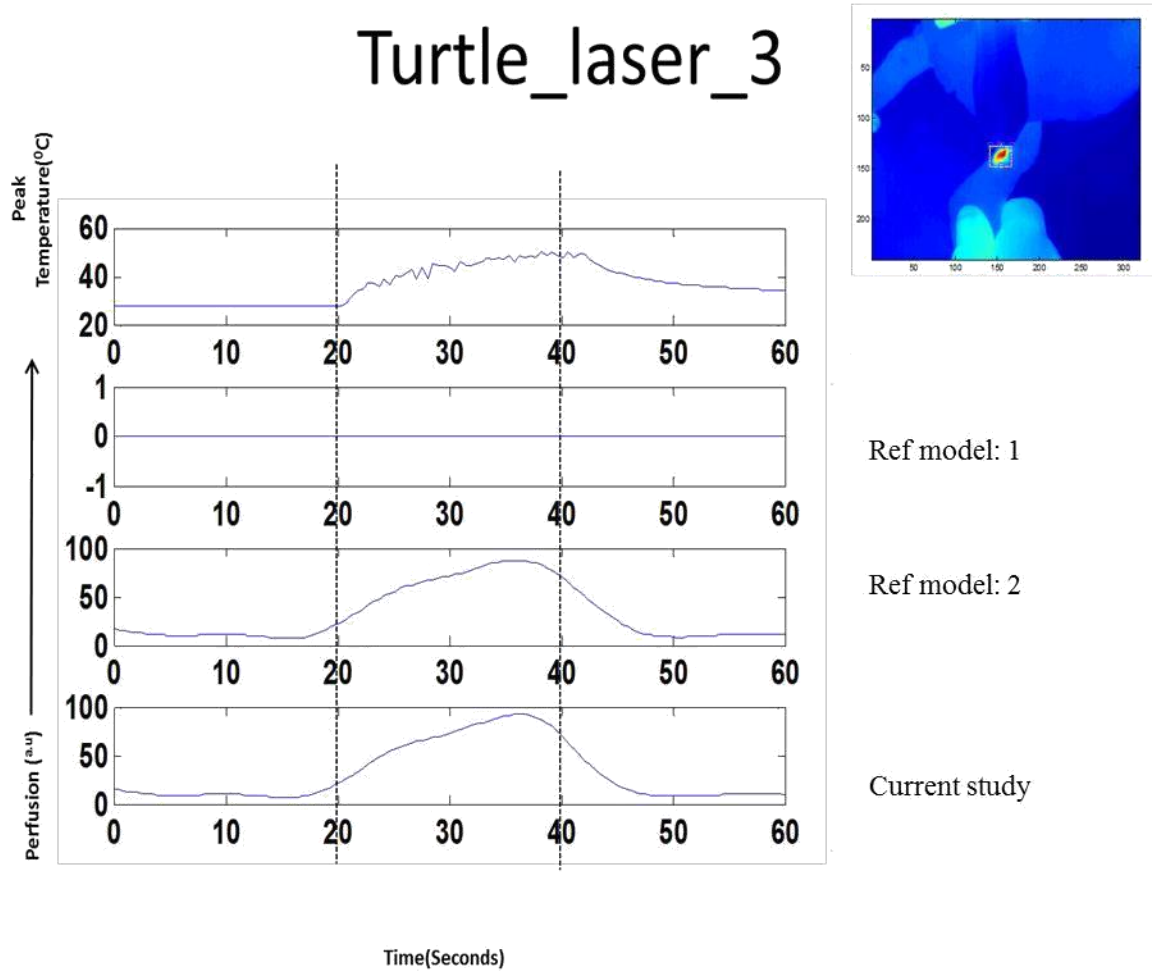


Figure 30: Temperature and Perfusion values from in-vivo data of turtle leg with laser application

The results obtained from this set of data shown in figure 30 show that:

Reference model: 1 displays a zero perfusion output value over the entire 60 second duration, irrespective of the laser application. In this case reference model: 2 and current study displays a similar stable perfusion pattern output showing significant change during laser irradiation period and stable changes otherwise.

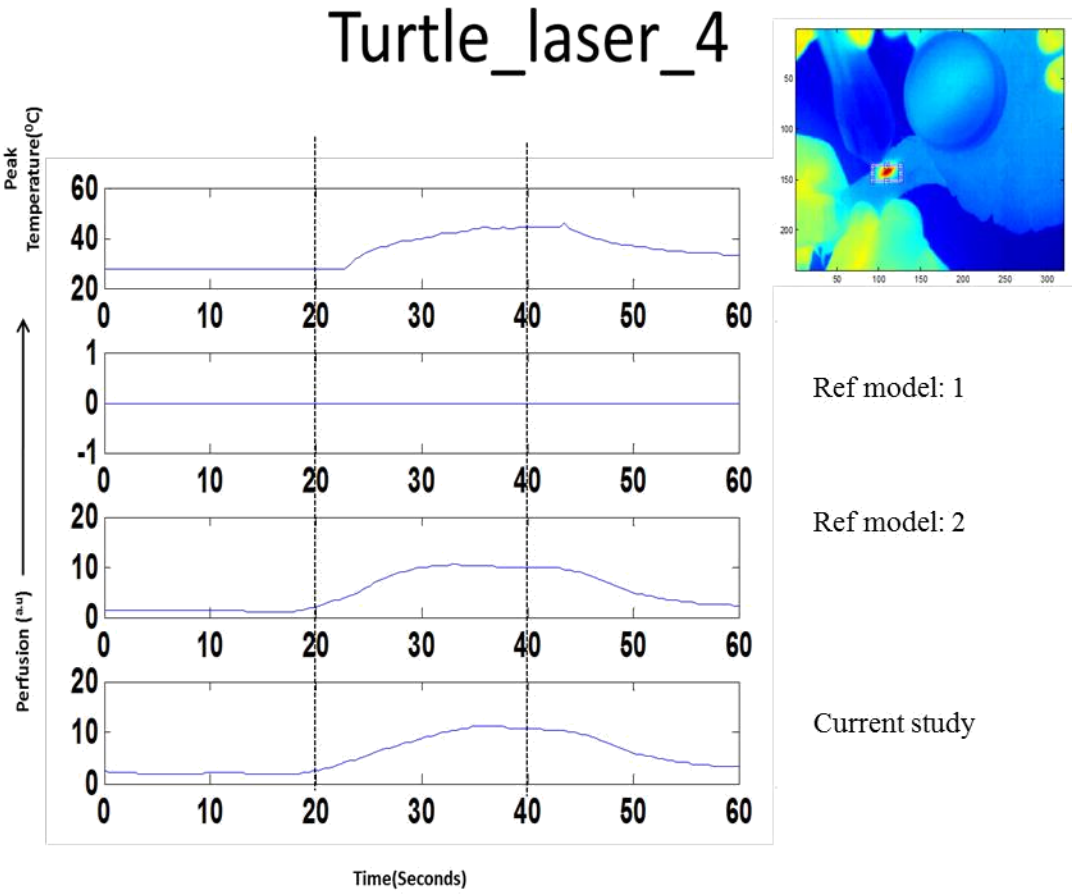


Figure 31: Temperature and Perfusion values from in-vivo data of turtle leg with laser application

The results obtained from this set of data shown in figure 31 show that:

Reference model: 1 displays a zero perfusion output value over the entire 60 second duration, irrespective of the laser application. In this case reference model: 2 and current study displays a similar stable perfusion pattern output showing significant change during laser irradiation period and stable changes otherwise.

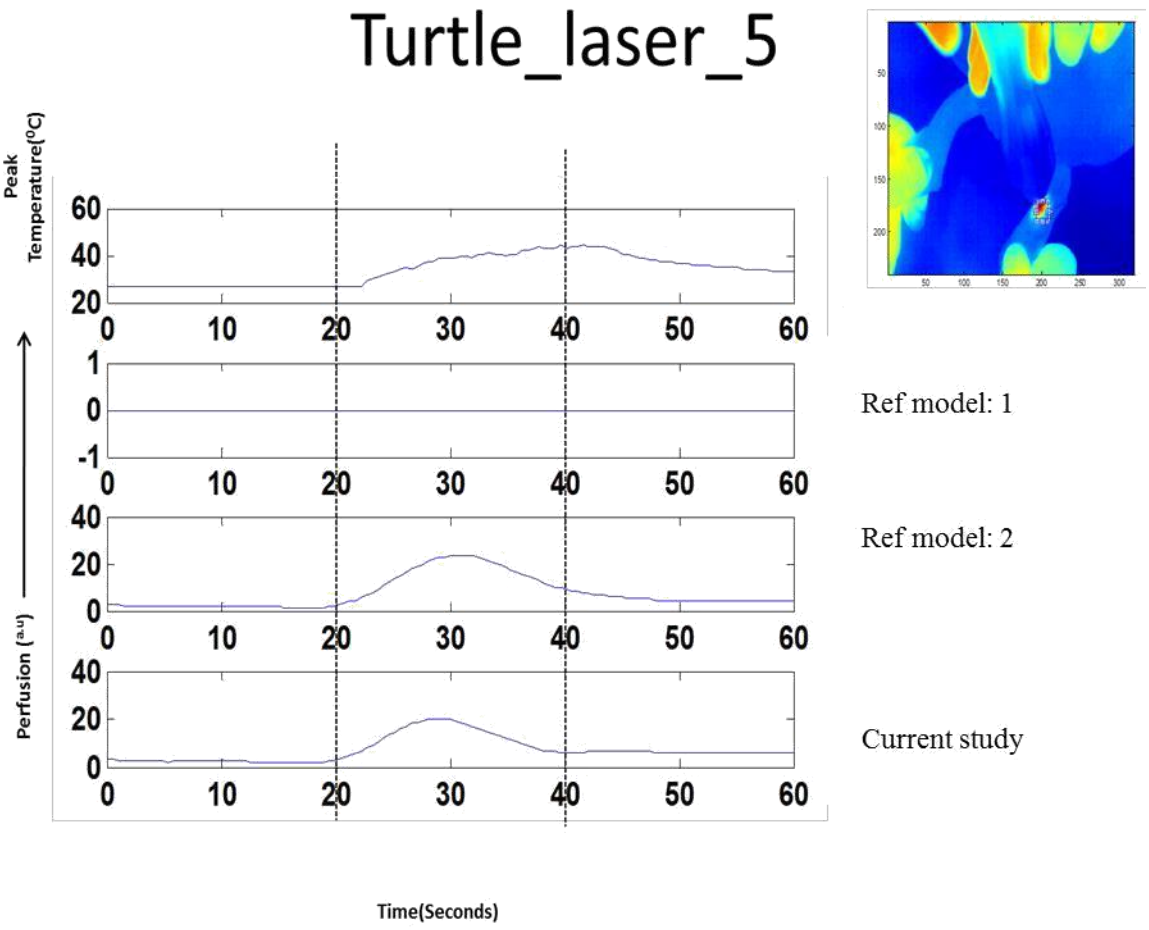


Figure 32: Temperature and Perfusion values from in-vivo data of turtle leg with laser application

The results obtained from this set of data shown in figure 32 show that:

Reference model: 1 displays a zero perfusion output value over the entire 60 second duration, irrespective of the laser application. In this case reference model: 2 and current study displays a similar stable perfusion pattern output showing significant change during laser irradiation period and stable changes otherwise.

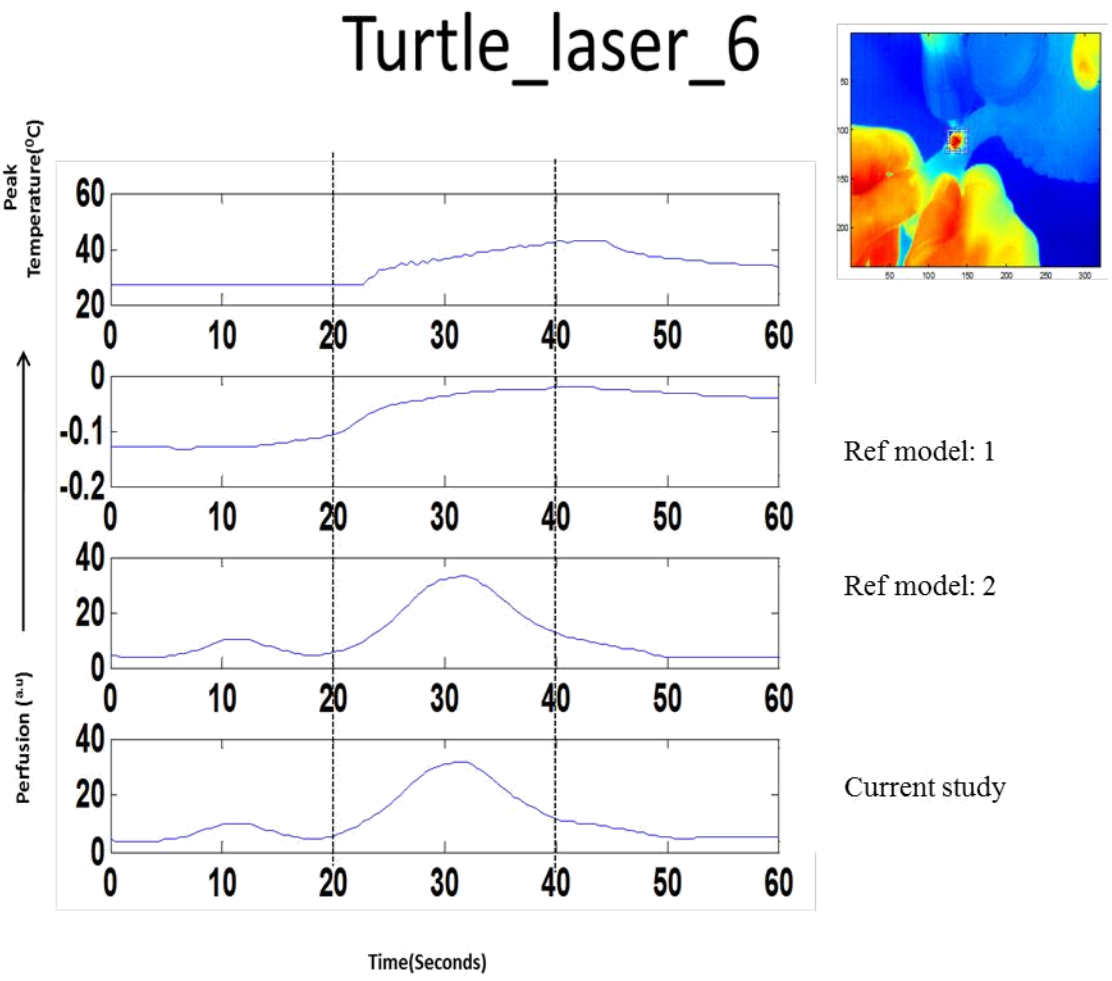


Figure 33: Temperature and Perfusion values from in-vivo data of turtle leg with laser application

The results obtained from this set of data shown in figure 33 show that:

Reference model: 1 displays a scaled temperature change pattern as the output perfusion pattern. In this case reference model: 2 and current study displays a similar stable perfusion pattern output showing significant change during laser irradiation period and stable changes otherwise.

iii. From Pressure Cuffing of Turtles legs.

Figures 34 to 41 shown below correspond to the outputs discussed above for 8 sets of data obtained by pressure cuffing both the legs of three turtles. The pressure cuffing protocol was implemented to observe the expected change of perfusion with the application and release of sudden pressure cuff.

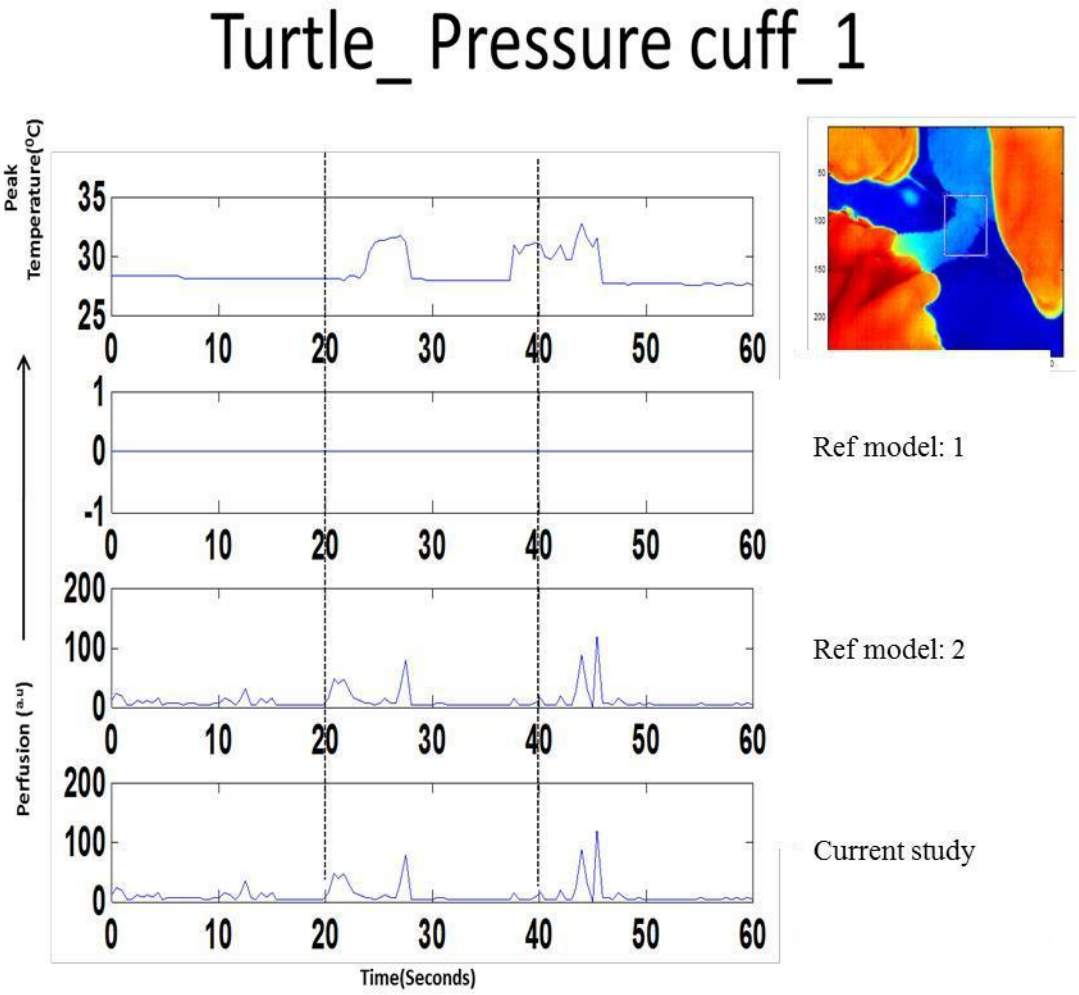


Figure 34: Temperature and Perfusion values from in-vivo data of turtle leg with the application of pressure cuff

The results obtained from all the sets of pressure cuffing data shown in figures 34 to figures 41 show that Reference model: 1 displays a zero perfusion output value over the entire 60 second duration irrespective of the application and release of cuff as it displays the perfusion pattern as a scaled temperature change rather than perfusion change. In this case reference model: 2 and current study displays a similar perfusion pattern output showing significant change during the application and release of pressure cuff and otherwise stable changes as expected.

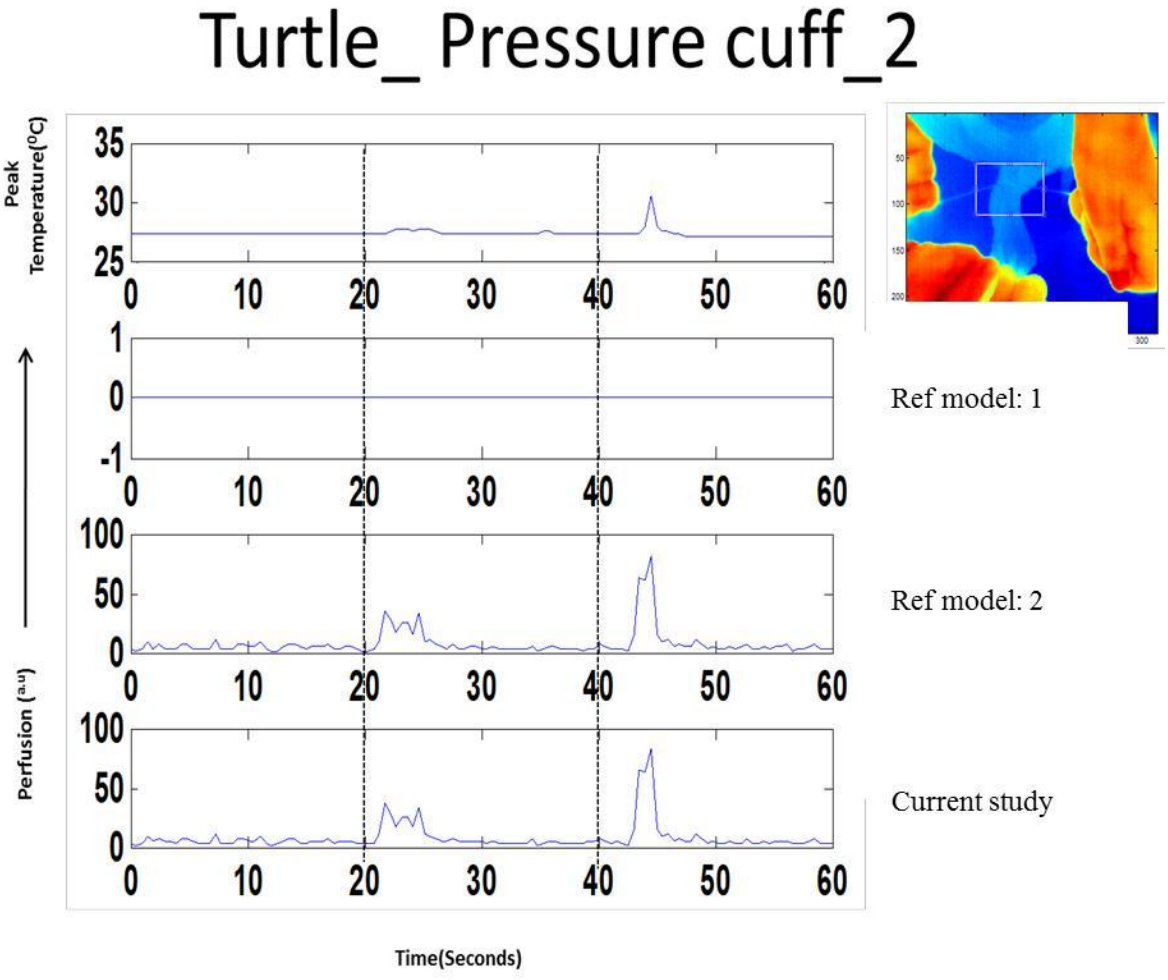


Figure 35: Temperature and Perfusion values from in-vivo data of turtle leg with the application of pressure cuff

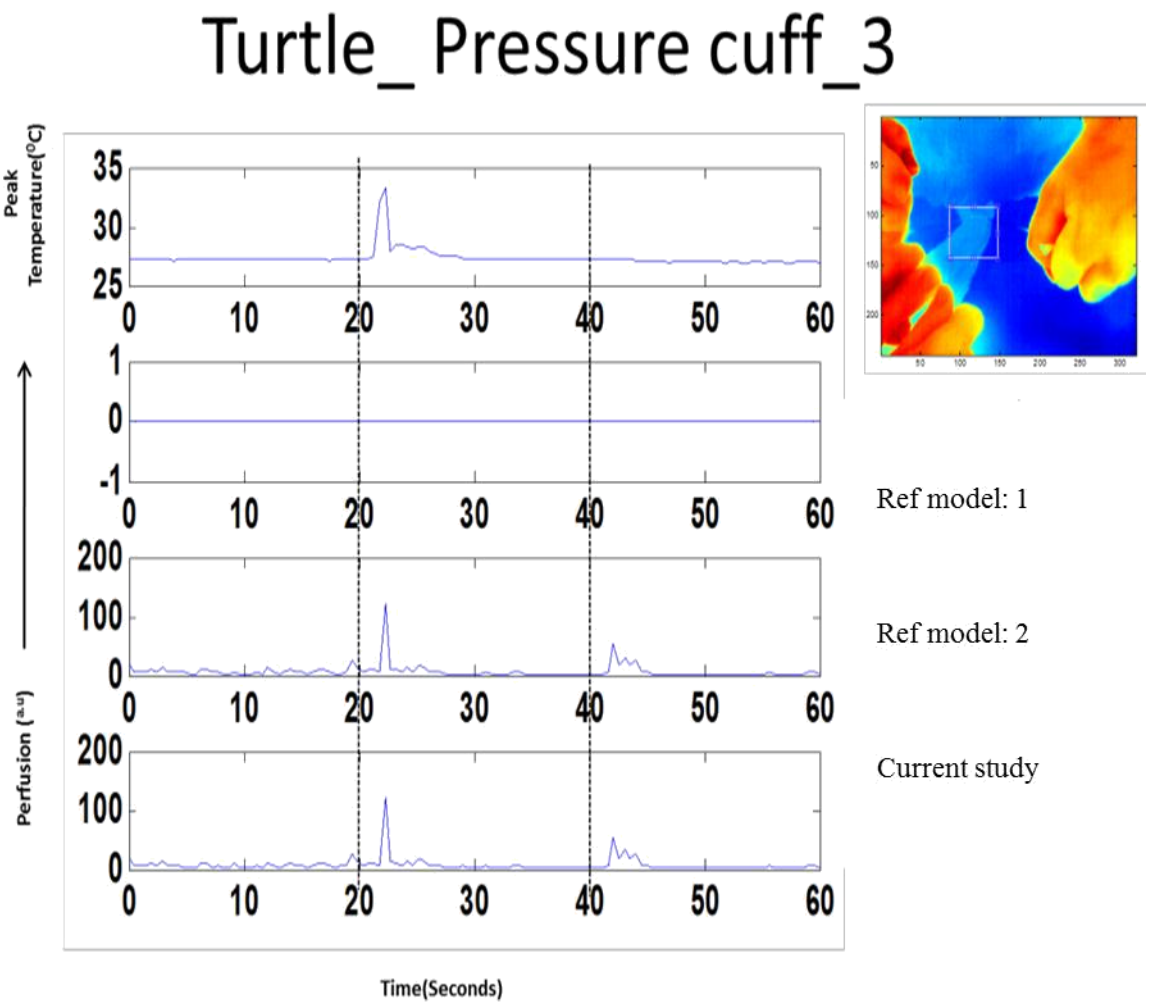


Figure 36: Temperature and Perfusion values from in-vivo data of turtle leg with the application of pressure cuff

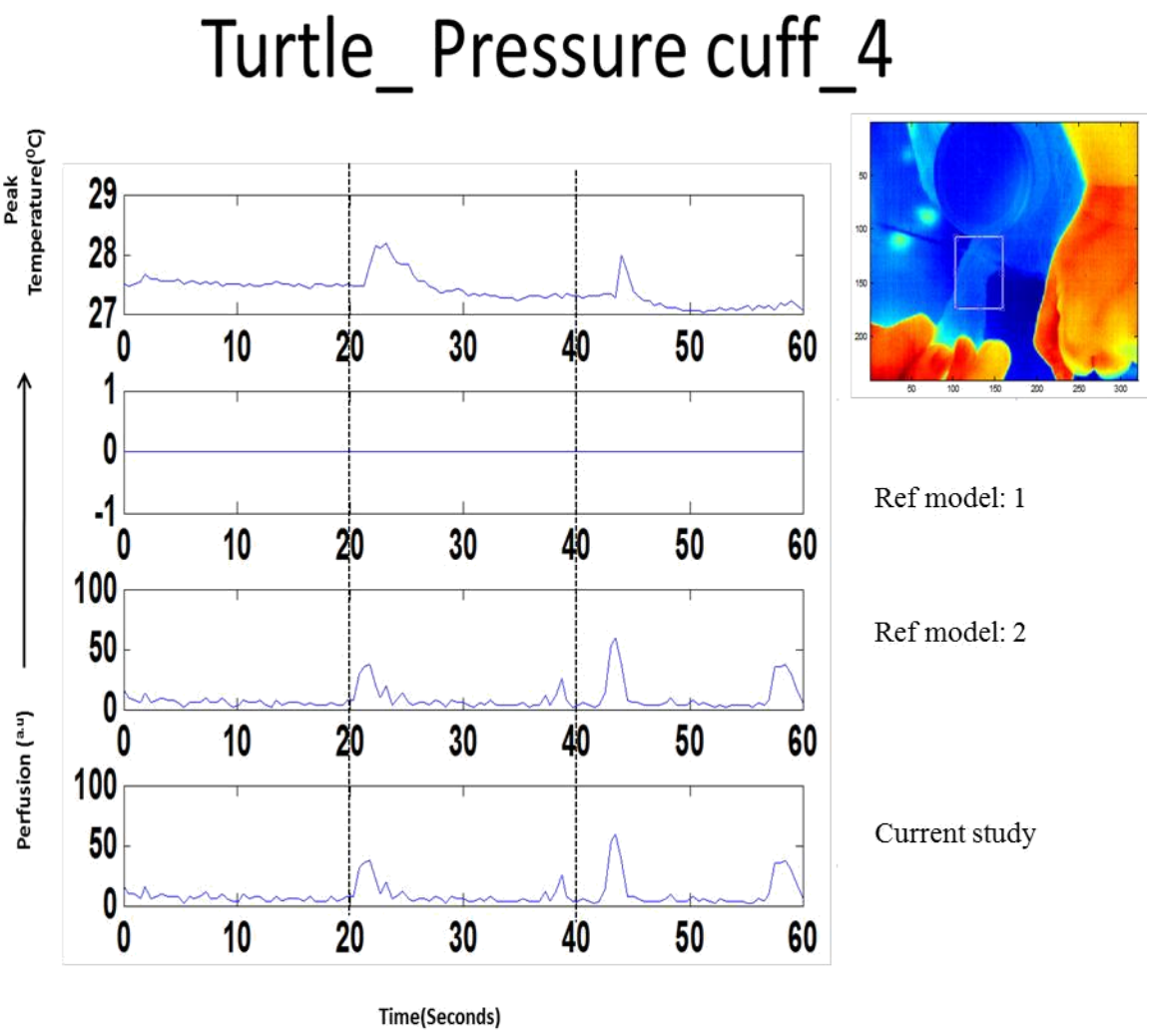


Figure 37: Temperature and Perfusion values from in-vivo data of turtle leg with the application of pressure cuff

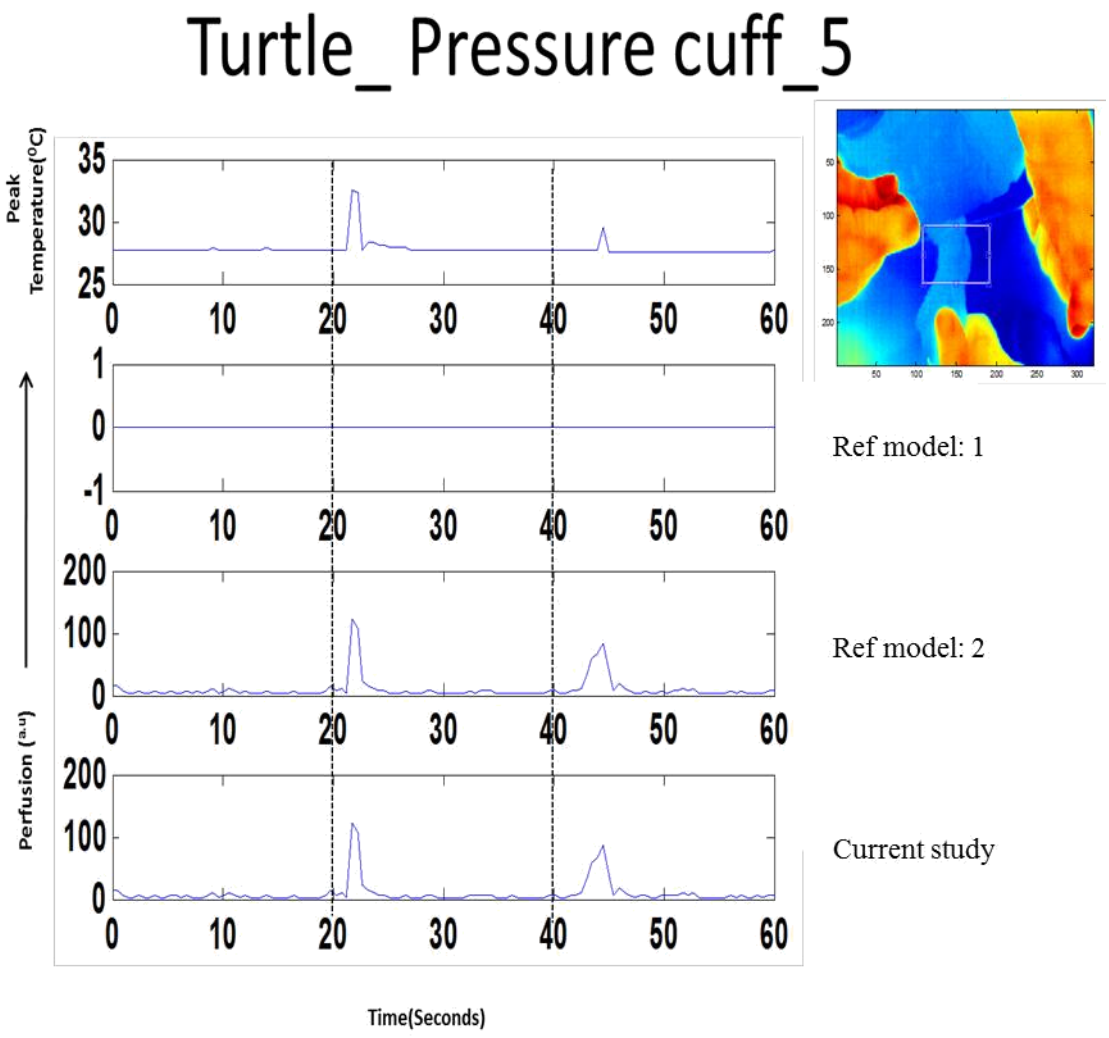


Figure 38: Temperature and Perfusion values from in-vivo data of turtle leg with the application of pressure cuff

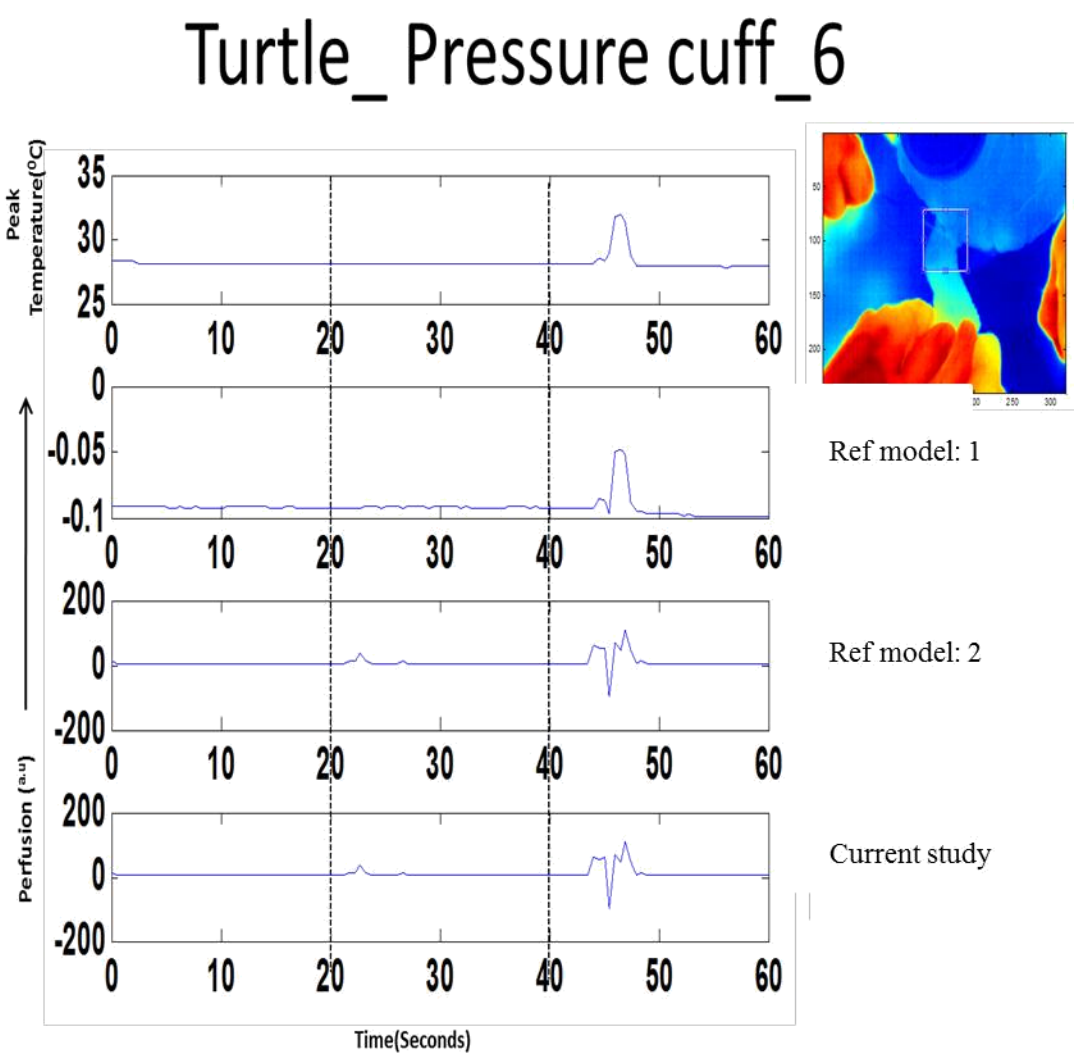


Figure 39: Temperature and Perfusion values from in-vivo data of turtle leg with the application of pressure cuff

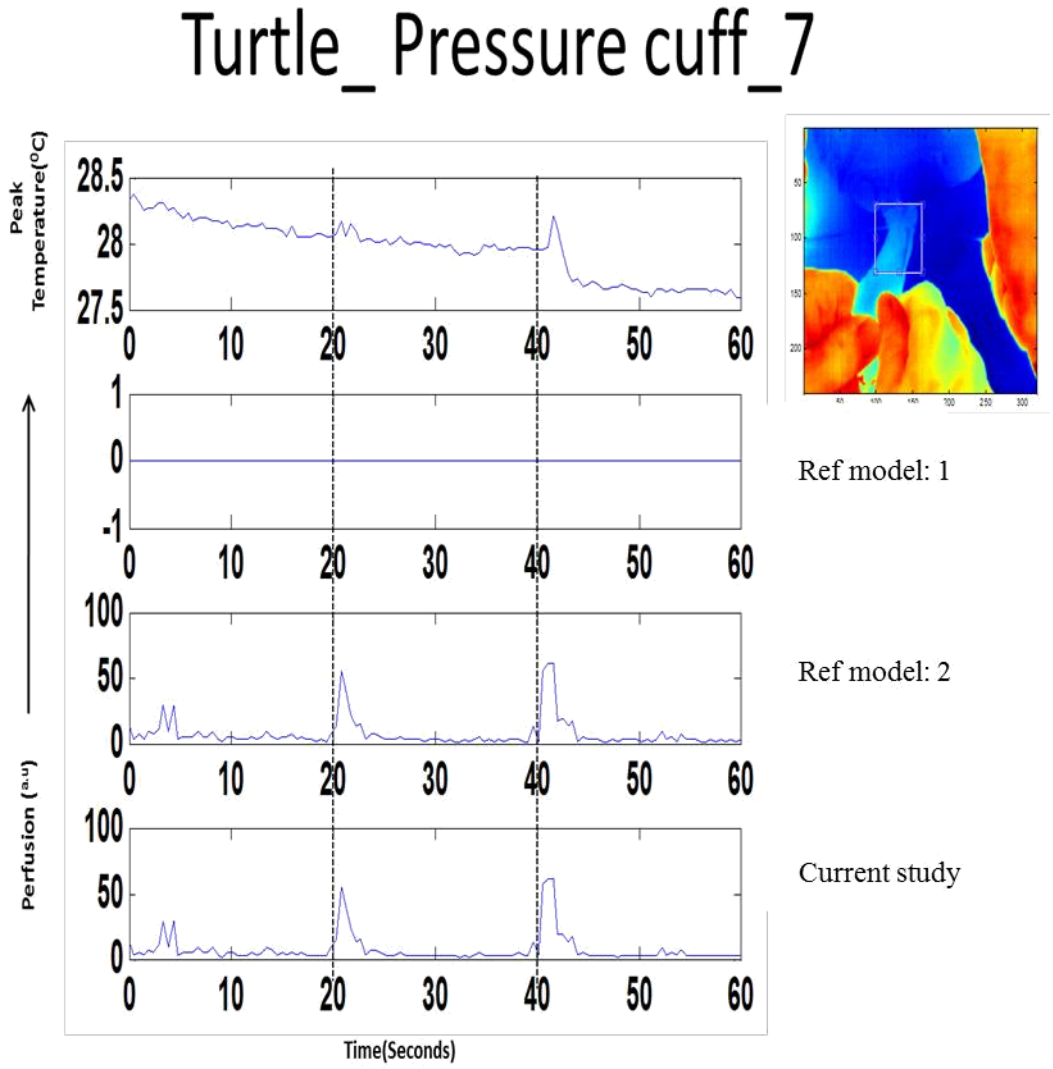


Figure 40: Temperature and Perfusion values from in-vivo data of turtle leg with the application of pressure cuff

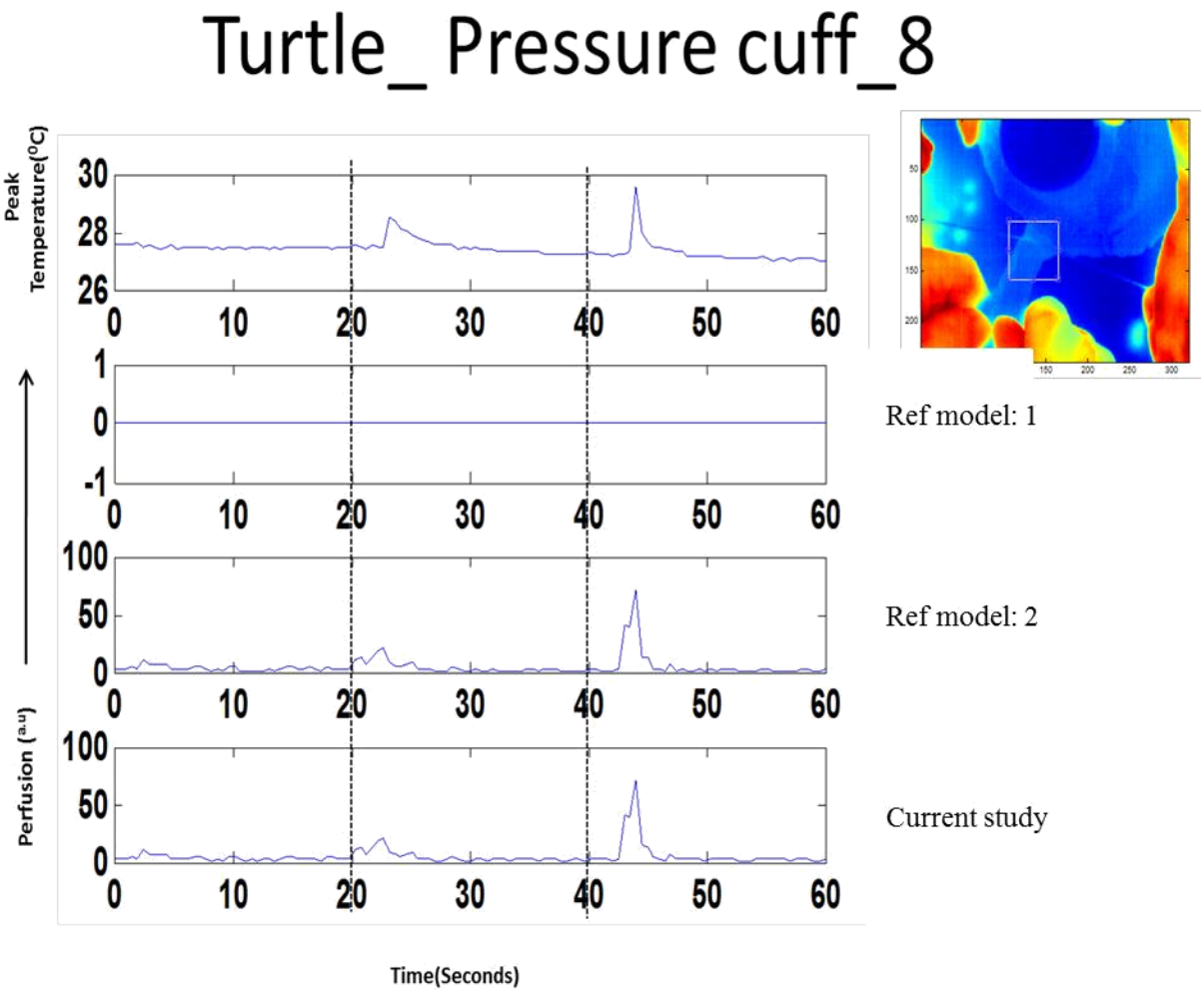


Figure 41: Temperature and Perfusion values from in-vivo data of turtle leg with the application of pressure cuff

## IV.3 Part-3

In this part of the study we are trying to compare the perfusion patterns that are obtained from our proposed model, with the same method that is discussed in the previous part i.e. part1, from data obtained with laser protocol over humans and turtle without using smoothing technique which was used in processing the data for part1. The perfusion pattern of endotherms and ectotherms due to thermal changes from [26] is shown below

in figure 42. This pattern is compared with the output pattern obtained from our study with the human and turtle data attributing to the endothermic and ectothermic nature of these species.

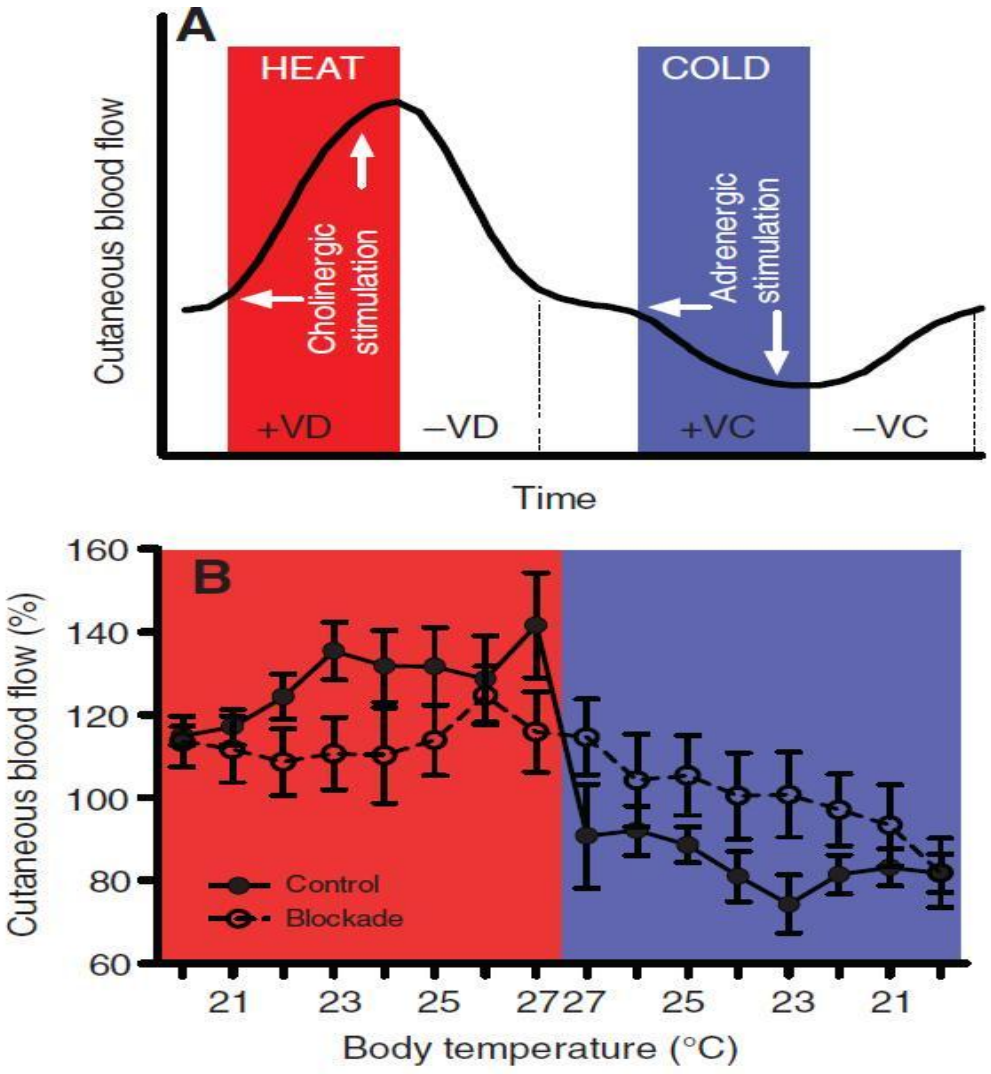


Figure 42: Perfusion patterns due to thermal variation (A) On Endotherms and (B) On Ectotherms from [25]

Figures 43 to 48 shown below compare the temperature changes and perfusion pattern of humans and turtles due to low-level laser irradiation.

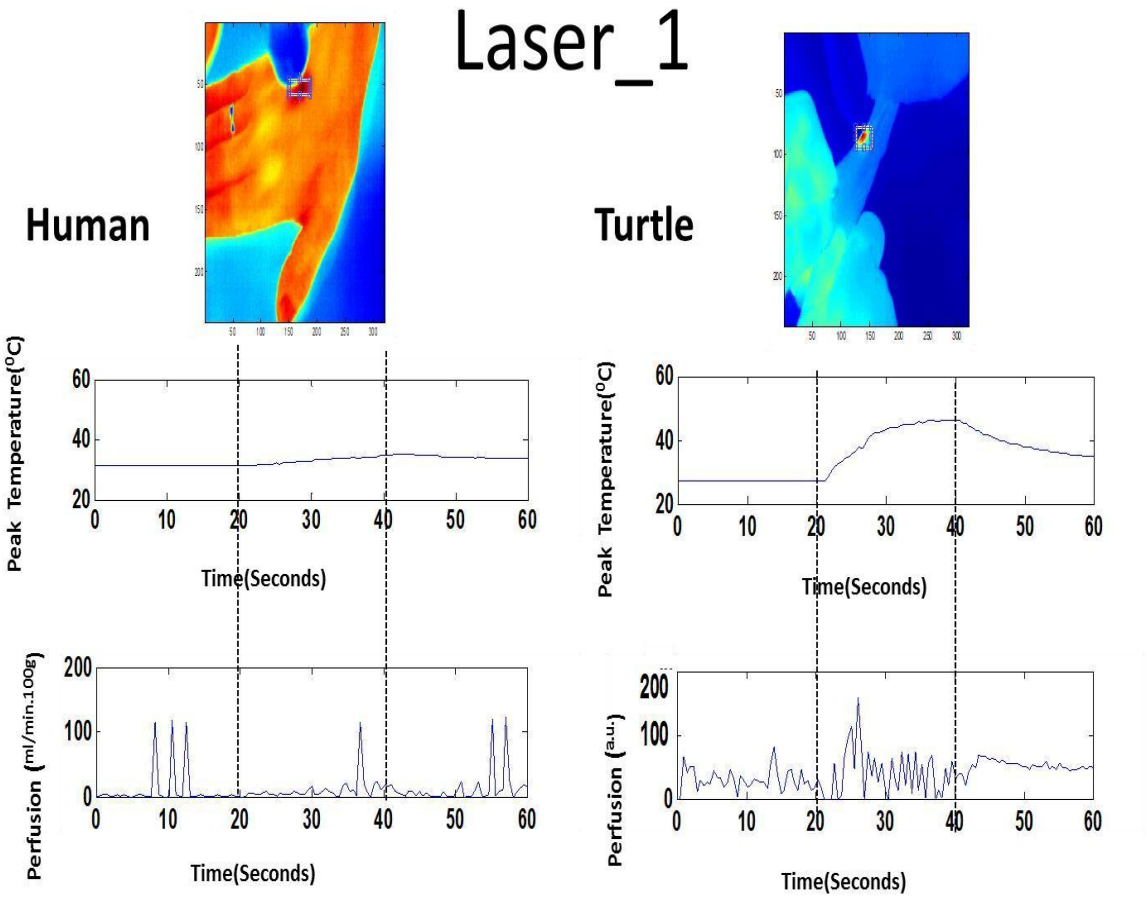


Figure 43: Comparing Temperature and Perfusion values from in-vivo data of human hand and turtle leg with laser irradiation

The results obtained from all the 6 sets of human and turtle data shown in figures 43 to figures 48 show that the temperature changes, due to laser irradiation in humans is much less when compared to that of turtles attributing to the adaptive thermogenesis of endotherms. The similarity between patterns from both the species is that there is an increase in perfusion with laser irradiation and the difference in the patterns occurs when

the laser is turned off. There is an abrupt decrease in perfusion for the turtle data and the decrease is not so abrupt in case of humans. The difference in perfusion patterns between human and turtle data may be attributable to the varying levels of vasodilation and vasoconstriction due to heat induced by laser irradiation.

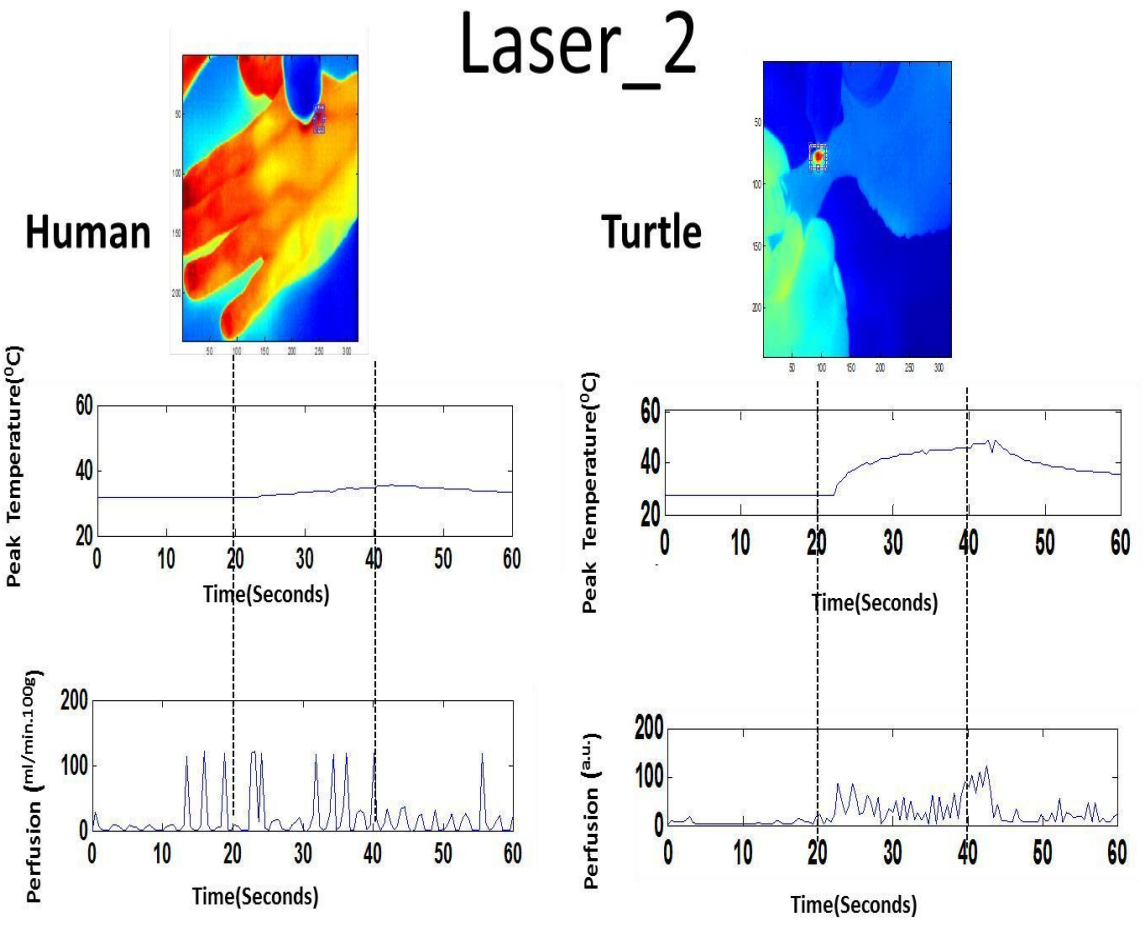


Figure 44: Comparing Temperature and Perfusion values from in-vivo data of human hand and turtle leg with laser irradiation

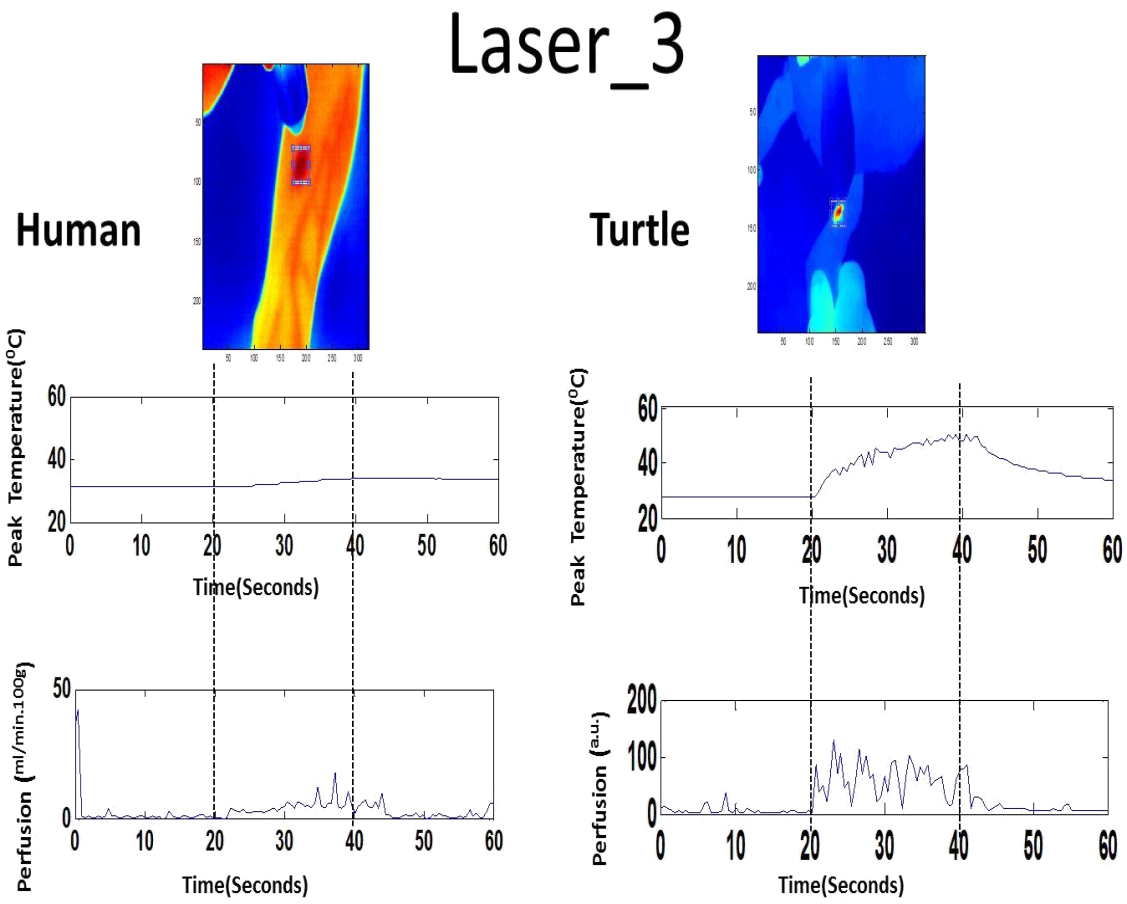


Figure 45: Comparing Temperature and Perfusion values from in-vivo data of human hand and turtle leg with laser irradiation

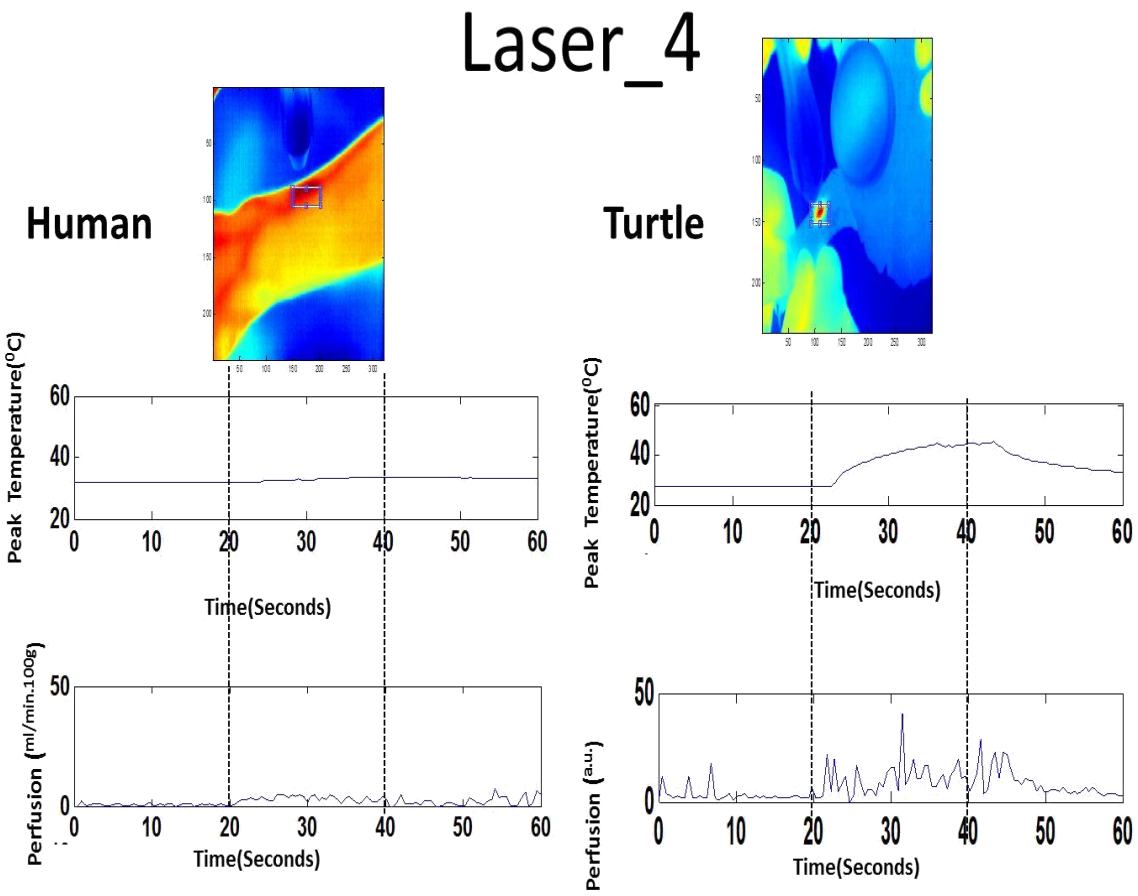


Figure 46: Comparing Temperature and Perfusion values from in-vivo data of human hand and turtle leg with laser irradiation

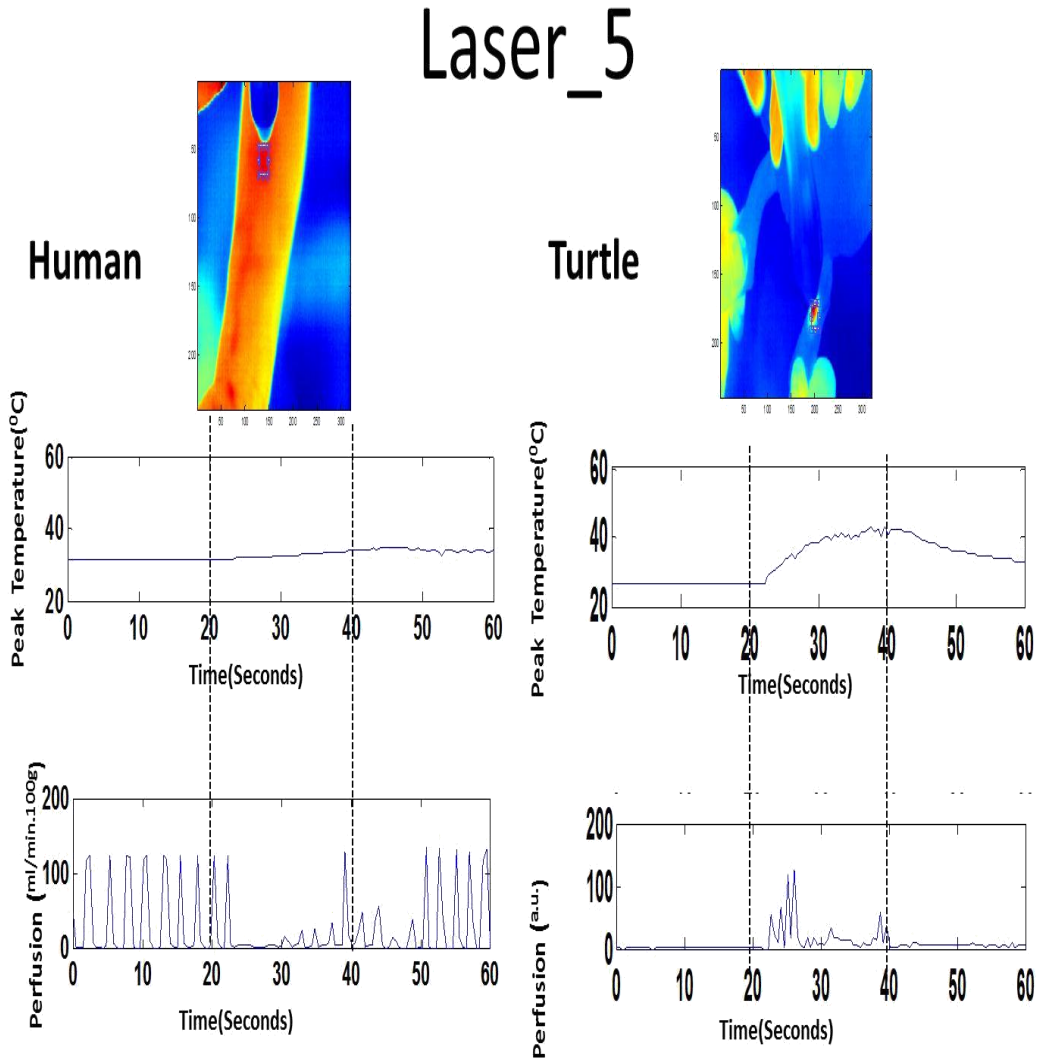


Figure 47: Comparing Temperature and Perfusion values from in-vivo data of human hand and turtle leg with laser irradiation

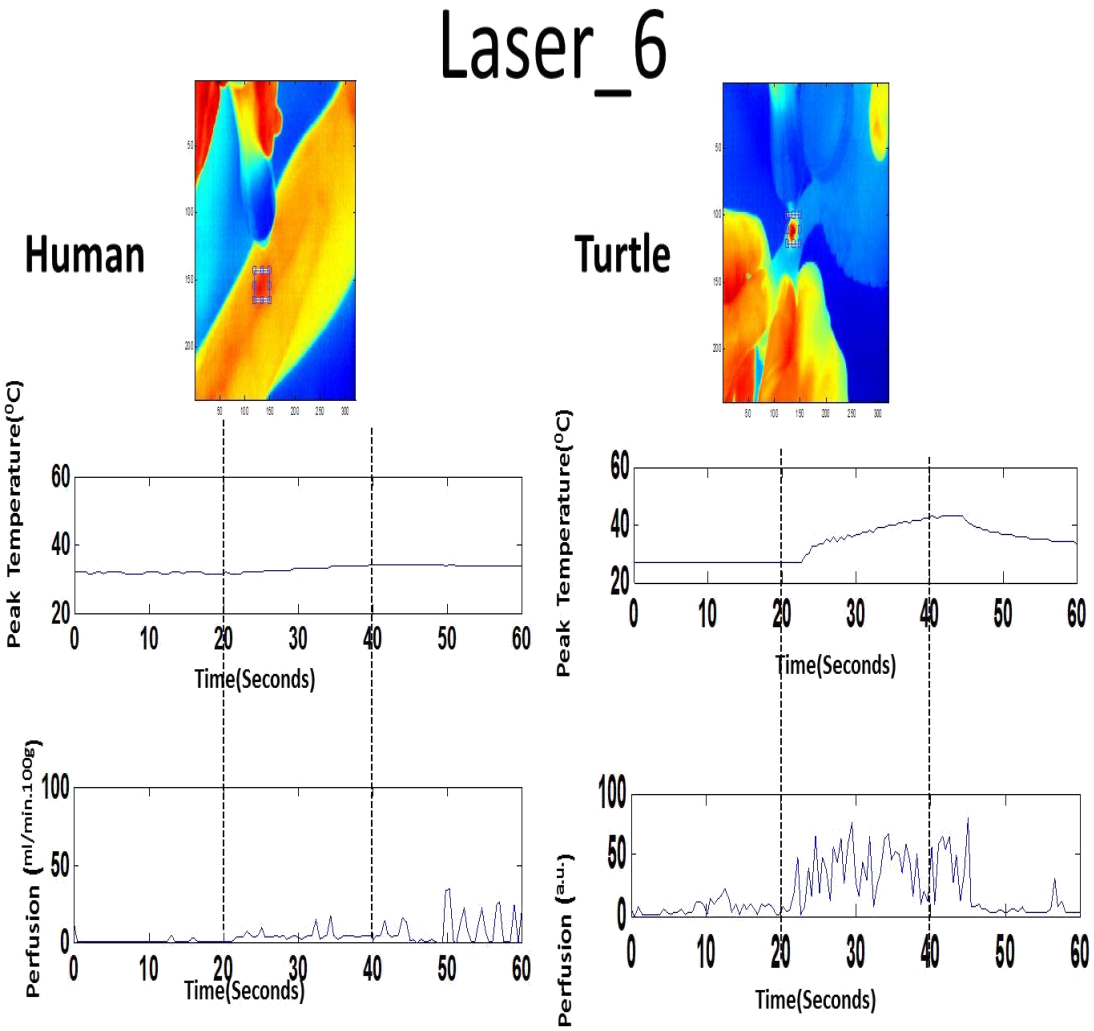


Figure 48: Comparing Temperature and Perfusion values from in-vivo data of human hand and turtle leg with laser irradiation

# CHAPTER V

## ONGOING, FUTURE WORKS & CONCLUSION

### V.1 Ongoing work - GUI for thermography derived perfusion imaging

A user-friendly Graphical-User-Interface (GUI) was developed in Matlab such that it can take several saved raw data thermal images, display the thermal maps, process them and display the processed perfusion output with an overlapped input thermal image.

This part of the work is aimed at helping the medical practitioners observe the temperature changes and the temperature derived perfusion changes of the subject. Shown below are snap shots to show the sequential working of the GUI.

Figure 49 shows the look of the user friendly GUI.

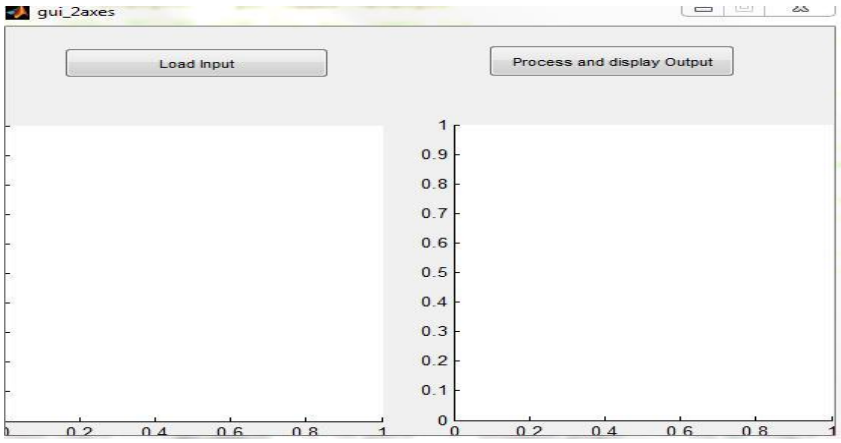


Figure 49: Snapshot of display of User friendly GUI

On clicking of the Load Input pushbutton, shown in figure 49, the interface asks to choose the folder with the data and the particular data that needs to be processed. This process is shown in figure 50.

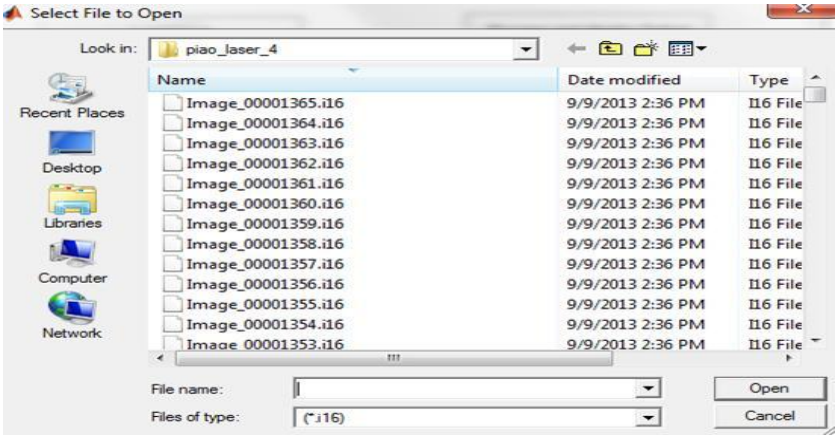


Figure 50: Snapshot of selecting input data in user-friendly GUI

Upon selecting the input the raw thermal data are loaded for visualising.

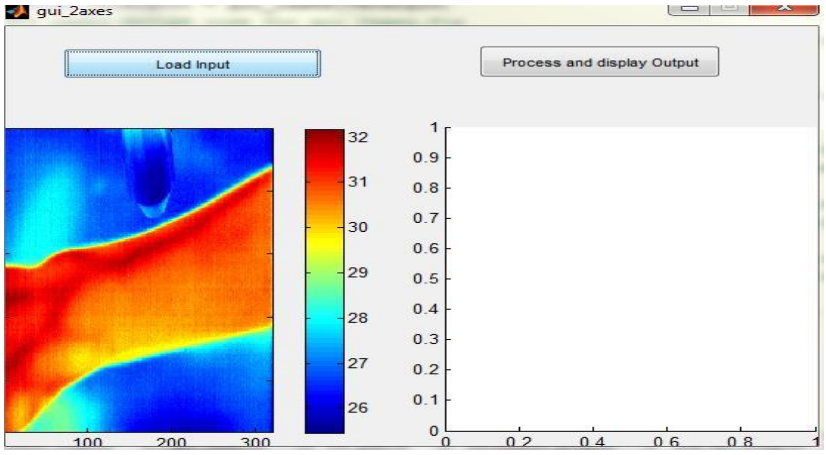


Figure 51: Input thermal images being displayed with a color bar

On clicking the process and display output pushbutton, shown in figure 51, the selected thermal data is processed and the Perfusion data Overlapped with the Thermal data with a transparency is displayed as output. This overlapping with transparency enables better

observing of the Temperature derived perfusion changes with the temperature changes. This output is shown in figure 52.

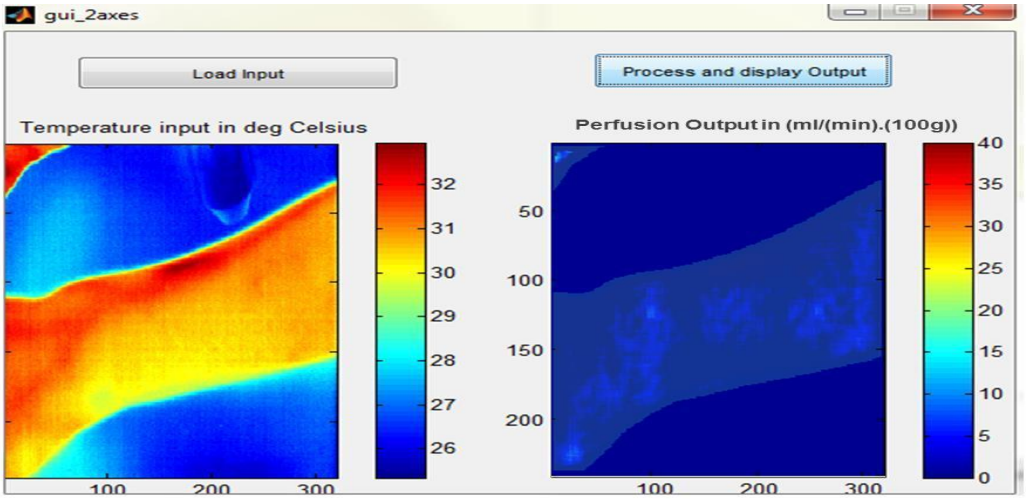


Figure 52: Perfusion output with an overlapped input with transparency

Then a movie file of the output perfusion images is created and saved as .avi file. This .avi file can be used on any system without additional software unlike the obtained input thermal images in their raw data format and the GUI which works on Matlab. Having these movie files saves a lot of time and effort when there is a need to access the perfusion output, as they do not need to be recomputed several times for the same set of data.

## V.2 Future Work

The current work involves developing and implementing an improved approximated bio-heat model for thermography derived perfusion from in-vivo data obtained from turtle subjects and human volunteer with low-level laser irradiation. However, in order to

quantitatively support the results a Synthetic study with true condition still needs to be implemented.

The experimental study to obtain in-vivo data can be implemented with better control which will be a challenging task but can possibly result in more informative and accurate results. The present work investigates the cutaneous perfusion response to low-level laser. In future the cutaneous perfusion response to different kinds of heat can be studied and compared. Also the modelling can be carried out at a more rigorous level by considering more factors resulting in further improvement in future.

The ongoing work involves the implementation of a user friendly GUI for thermography derived imaging. The present GUI takes several saved raw data thermal images, display the thermal maps, process them and display the processed perfusion output with an overlapped input thermal image and also displays the output images as movie files. There is scope to improve this GUI by making its implementation real-time instead of working with saved thermal images. Also there is possibility of including customized functions with the GUI implementation according to the needs of the medical practitioners.

## V.3 Conclusion from Results

Perfusion is important to the healthy functioning of the body and therefore its quantification can be of great use to medicine and health care. Also with Low-level laser therapy playing a significant role in medical treatment, it has become important to understand how the tissue will thermally respond during treatments allowing physicians to plan treatment doses and durations for the procedures. Previous studies have demonstrated that Temperature derived perfusion can be derived from dynamic

thermography imagery by applying bio-heat transfer models. In this study we develop a bio-heat transfer model for deriving perfusion information from thermography imagery along the same basis but with fewer approximations than the referred previous studies.

In this study different models from other studies and our developed model are used to process sets of real time thermal images obtained from our study to observe the pattern of perfusion changes with low-level laser irradiation. As part of this process there was a temperature elevation due to laser irradiation. This procedure was based on the fact that an increase in heat flux from the unheated state will raise the tissue temperature sufficiently to cause capillary recruitment and vasodilation. From the results of the procedure of lased data by reference model: 2 and current study there is an agreement about the increased perfusion pattern over the lased region for the specific duration of 20seconds to 40 seconds. However the degree of variation differs from data to data as expected. The first model from reference model: 1 followed the pattern of temperature changes. The perfusion pattern of their model is similar to a scaled temperature pattern of the input data rather than perfusion pattern. Current study gives a similar perfusion pattern for all the sets of lased human data whereas reference model: 2 falters in certain cases. This happens when the data contains laser head, any sharp edges, or significant artefacts with a high temperature, where selective thresholding is not applicable as it interferes with the range of required information. In such situations the former model shows drastic changes in the perfusion pattern whereas our model gives a stable perfusion pattern similar to the data without interferences. This improvement can be attributed to the additional laplacian term involved in the model in current study.

For the lased turtle data the output perfusion pattern from reference model: 2 and current study yields similar results. Also for the pressure cuffed data from turtle legs, an increase in perfusion during the sudden pressure cuff variation and stable perfusion at other times was observed from reference model: 2 and current study .The similar perfusion pattern between the two methods may be due to the likely low changes due to heat conduction by the subcutaneous tissue attributable to their thermoregulation mechanism. Without significant changes due to this parameter the additional improvements in our model do not have any significant effect thereby giving a similar output when compared to the former model.

When comparing the results obtained from the laser procedure of human and turtle data it is observed that that the temperature changes, due to laser irradiation in humans is much less when compared to that of turtles attributing to the adaptive thermogenesis of endotherms. There is an increase in perfusion due to laser irradiation and decrease in perfusion when the laser is turned off for both the species. But the decreasing perfusion pattern is different for humans and turtles. There is an abrupt decrease in perfusion for the turtle data and the decrease is not so abrupt in case of humans. The difference in the decreasing perfusion patterns between human and turtle data may be attributable to the varying levels of vasodilation and vasoconstriction due to heat induced by laser irradiation between endotherms (humans) and ectotherms (turtles).

# REFERENCES


1. Lin, W., Liauh, C., Chen, Y., Liu, H., Shieh, M., 2000, "Theoretical study of temperature elevation at muscle/bone interface during ultrasound hyperthermia," Medical Physics, Vol. 27, No. 5, pp. 1131-1140.
2. Optical-thermal Response of laser Irradiated Tissue, edited by A. J. Welch and M. J. C. van Gemert, Plenum press, New York, 1995.
3. Ying-Ying Huang, Michael Hamblin, and Aaron C.-H. Chen**, "**Low-level laser therapy: an emerging clinical paradigm", Biomedical Optics & Medical Imaging, SPIE Newsroom, DOI: 10.1117/2.1200906.1669, 9 July 2009.
4. Light propagation modelling using Comsol Multiphysics, Medical Optics Course Atomic Physics Lund University.
5. Gayzik, F.S., 2004, "Optimal control of thermal damage to biological tissue," Masters thesis, Mechanical Engineering, Virginia Tech.
6. Madden, 2004 "A non-clinical method to simultaneously estimate thermal conductivity, volumetric specific heat, and perfusion of in-vivo tissue ," Masters thesis, Mechanical Engineering.
7. Lokshina, A. M., Song, C. W., Rhee, J. G., and Levitt, S. H. (1985). "Effect of fractionated heating on the blood flow in normal tissues." *International Journal of Hyperthermia*, 1(2), 117-129.

8. Urbanavičius L, Pattyn P, Van de Putte D, Venskutonis D, "How toassess intestinal viability during surgery: A review of techniques." *World J Gastrointest Surg* 2011; 3(5): 59-69

9. R. A. London1, J. Eichler1,2, J. Liebetrudt3, L. Ziegenhagen , "Design of a protocol for combined laser hyperthermia–photodynamic therapy in the esophagus", Proceedings of Lasers in Surgery: Advanced Characterization, Therapeutics, and Systems, Bellingham, WA, January 22-23, 2000

10. Erin Heng-Yu Liu, "Tissue and Cellular Responses to Chronic *In vivo* Heating", Thesis for doctor of ohilosophy , Department of Biomedical Engineering, Case Western Reserve University

11. Johannes Johansson, "Impact of Tissue Characteristics on Radio_Frequency Lesioning and Navigation in the Brain-*Simulation, experimental and clinical studies",* Linköping Studies in Science and Technology Dissertation No. 1230

12. Mayrovitz, Regan, "Gender difference in Facial Skin Blood Perfusion during Basal and heated condition determined by Laser Doppler Flowmetry", microvascular research 45, 211-218(1993)

13. Catherine E. Kang,1,2 Richard Clarkson,3 Charles H. Tator,4 Ivan W.T. Yeung,3,5 and Molly S. Shoichet, "Spinal Cord Blood Flow and Blood Vessel Permeability Measured by Dynamic Computed Tomography Imaging in Rats after Localized Delivery of Fibroblast Growth Factor", Journal of Neurotrauma 27:1–12 (November 2010) Mary Ann Liebert, Inc.DOI: 10.1089/neu.2010.1345

14. Guoqiang Yu, Thomas F. Floyd, Turgut Durduran , Chao Zhou1, Jiongjiong Wang, John A. Detre, Arjun G. Yodh1, "Validation of diffuse correlation

spectroscopy for muscle blood flow with concurrent arterial spin labeled perfusion MRI", 2007 Optical Society of America

15. Nishimoto, Ishiura "Effects of Ultrasonic Radiation on cutaneous blood flow in the paw of Decerebrated Rats", Kawasaki Journal of Medical Welfare VOl.12, No.1, 2006 13-18
16. A. Merla, S. Di Romualdo, L. Di Donato, M. Proietti, F. Salsano and G. L. Romani, "Combined Thermal and Laser Doppler Imaging in the Assessment of Cutaneous Tissue Perfusion", Proceedings of the 29th Annual InternationalConference of the IEEE EMBSCité Internationale, Lyon, France,August 23-26, 2007.
17. Ioannis Pavlidis ,James Levine, "Thermal Image Analysis for Polygraph Testing", IEEE Engineering in Medicine and Biology 2002
18. lwao Fujimasa, Tsuneo Chinzei,ltsuro Saito ,"Converting Far Infrared Image Information to other Physiological data", IEEE Engineering in Medicine and Biology 2000
19. Iwao Fujimasa Tsuneo Chinzei and Kunihiko Mabuclzi **,"**Converting Algorithms for Detecting Physiological Function Changes from Time Sequential Thermal Images of Skin Surface**",** 1995 IEEE-EMBC and CMBEC
20. M. Iwatani "An estimation method of skin blood flow rate using heat flow analysis", *Jap. J. Medical Electron. Biologic. Eng.*, vol. 20, no. 3, pp.249 -255 1982

21. ShiqianWu,Weisi Lin, Shoulie Xie, "Skin heat transfer model of facial thermograms and its application in face recognition", 2008 Elsevier Ltd.doi:10.1016/j.patcog.2008.01.003

22. http://personal.cityu.edu.hk/~bsapplec/heat.htm

23. Christian Sturesson," Medical Laser-Induced Thermotherapy Models and Applications" Lund Reports on Atomic Physics LRAP-235, ISBN 91-628-3134-8.

24. N. Otsu, "A threshold selection method from gray-level histograms," IEEE Trans. Syst. Man Cybern. **9**(1), 62–66 (1979).

25. Frank Seebacher, "Responses to temperature variation: integration of thermoregulation and metabolism in vertebrates", The Journal of Experimental Biology 212, 2885-2891, doi:10.1242/jeb.024430

26. Shaun F. Morrison, Kazuhiro Nakamura and Christopher J. Madden, "Central control of thermogenesis in mammals", *Exp Physiol* 93.7 pp 773–797

27. Jeffery M. Morrissette*, Jens P. G. Franck† and Barbara A. Block, "Characterization of ryanodine receptor and Ca2+-ATPase isoforms in the thermogenic heater organ of blue marlin (Makaira nigricans)", The Journal of Experimental Biology 212, 2885-2891, doi:10.1242/jeb.00158

28. http://www.nature.com/scitable/popular-discussion/1115

29. http://www.nature.com/scitable/knowledge/library/homeostatic-processes-for-thermoregulation-23592046

# APPENDICES

```
% To process raw thermal data in matlab.

close all;

clear all;

clc;

 [filename pathname] = uigetfile('*.i16', 'multiselect','on');

dirname = uigetdir;

files = dir(dirname);

fileIndex = find(~[files.isdir]);


for i=3:(numel(fileIndex)-2) filename
    = files(fileIndex(i)).name;

    fid = fopen([pathname

    filename],'r+'); LgthFileMainHeader

    = 3476; LgthImHeader = 1016;

    fseek(fid, 2, 'bof');

    NbRowImage = fread(fid,1,'uint16');

      fseek(fid, 4, 'bof');

    NbColImage = fread(fid,1,'uint16');

    fseek(fid, 8, 'bof');
```

```
B{i} = fread(fid, [NbRowImage,NbColImage] ,'uint16' );
    a{i} = double(B{i});
    a{i}=imrotate(a{i},270);
    a{i}= a{i}/100;
    fclose('all');
    figure;
    imagesc(a{1});
    impixelinfo;
end
% To select one frame out of every 10 frames and process the
model for i=1:10:(numel(fileIndex)-2)
    in_old{i}=a{i};
    in=in_old(~cellfun('isempty',in_old));
end
for i=1:(max(size(in)))
G = fspecial('average',[8,8]);
  in_2{i}= imfilter(in{i},G,'same');
end
% To apply selective thresholding
x=in_2;
for i=1:numel(in)
for k= 1:240
for l=1:320
```

```
        if x{1,i}(k,l)<26
            x{1,i}(k,l)=0;
        end
    end
end
end
%%
for i=1:(numel(in))
    Iedge{1,i}=edge(x{1,i});
    IedgeD{1,i}=imdilate(Iedge{1,i},ones(7));
    Itemp=IedgeD{1,i};
    IedgeD{1,i}=~Itemp;
end
for i=1:(numel(in)-1)
    dtsbydt{i}=double((x{i+1}-x{i}));
end
for i=1:(numel(in)-1)
h = fspecial('laplacian',0.2);
dts2bydt2{i}=
imfilter(x{i},h,'same'); end
% The parameter values from literature related to bio-heat model and modeling.
ptissue=1.01*10^-3;
ctissue=3600;
```

```
k=0.54;
pblood=1.06*10^-
3; cblood=3780;
tcore=37;
for j=1:(numel(in)-2)
  tempdiff{j}=double(tcore-x{j});
  iperf{j}=(ctissue.*dtsbydt{j})./(pblood*cblood.*(double(tcore-
  x{j}))); y{j}=k.*dts2bydt2{j};
z{j}=pblood*cblood*ptissue*tempdiff{j};
intermed{j}=(y{j}./z{j});
wb{j}=iperf{j}+intermed{j};
 op{j}=double(wb{j}.*IedgeD{j});
 figure;
  imagesc(op{j});
  caxis([0,40]);
  colorbar;
end
end
```

VITA

Vasumathi Chalasani

Candidate for the Degree of

Master of Science

Thesis: DYNAMIC THERMOGRAPHY DERIVED PERFUSION AS A POTENTIAL TOOL TO EVALUATE CUTANEOUS PERFUSION CHANGES IN RESPONSE TO LOW-LEVEL-LASER IRRADIATION

Major Field: Electrical and Computer Engineering

Biographical:

Education:

Master of Science in Electrical and Computer Engineering at Oklahoma State University, Stillwater, Oklahoma in May, 2014.

Bachelor of Science in Electronics and Communication Engineering at Jawaharlal Nehru Technological University, Hyderabad, India in May, 2012.